Assessment of the Refined Zigzag Theory for bending, vibration, and buckling of sandwich plates: a comparative study of different theories

Assessment of the Refined Zigzag Theory for bending, vibration, and buckling of sandwich plates: a comparative study of different theories

L. Iurlaro[a,*] , M. Gherlone[a], M. Di Sciuva[a] and A. Tessler[b]

[a] Departement of Mechanical and Aerospace Engineering
Politecnico di Torino, Corso Duca degli Abruzzi 24, 10129 Torino, Italy
luigi.iurlaro@polito.it, marco.gherlone@polito.it, marco.disciuva@polito.it

[b] Structural Mechanics and Concepts Branch
NASA Langley Research Center, Mail Stop 190, Hampton, Virginia, 23681 – 2199, U.S.A.
alexander.tessler-1@nasa.gov

Abstract. *The Refined Zigzag Theory (RZT) belongs to the zigzag class of approximations for the analysis of laminated composite and sandwich structures. This paper presents the derivation of the non-linear equations of motion and consistent boundary conditions of RZT for multilayered plates. Subsequently, the equations are specialized to the linear boundary value problem of bending and the linear eigenvalue problems of free vibrations and buckling. In order to assess the accuracy of RZT, results concerning the static response, the free vibration frequencies and modal shapes, and the buckling loads of symmetric and un-symmetric sandwich plates, both simply supported and clamped and subjected to several loading conditions, are compared to the three-dimensional exact elasticity solution, high-fidelity FEM solutions, classical and zigzag theories, and accurate layer-wise models or solutions obtained in the open literature by means of other methods. The numerical investigation shows that RZT is highly accurate in predicting the static response, the natural frequencies and the buckling loads of sandwich plates without requiring any shear correction factors. In virtue of its accuracy and of the C^0 –continuity requirement for shape functions, RZT can be adopted to derive reliable and computationally efficient finite elements suited for large-scale analyses of sandwich structures.*

Keywords: sandwich plate, free vibration, buckling, Refined Zigzag Theory, shear correction factor

* Corresponding Author: Luigi Iurlaro, email: luigi.iurlaro@polito.it

1. Introduction

In the last decades, composite materials have been increasingly used in different engineering fields (military and civilian aircrafts, aerospace vehicles, naval and civil structures) due to their high stiffness-to-weight and strength-to-weight ratios. Sandwich structures show further remarkable characteristics in terms of impact energy absorption and noise reduction.

The classical sandwich-type construction is made of three layers (*ordinary sandwich*): the two external layers, called *skins* or *faces* or *face-sheets*, are separated by a thicker layer, called *core*. Generally, skins are made up of high-strength materials like steel or aluminum; however, to achieve higher stiffness- and strength-to-weight ratios, metallic materials are often substituted by composite materials. The core layer is made of a light material, which is usually much more compliant than the face-sheets. The three more typical geometries for the core are: honeycomb, corrugated, and cellular [1].

According to the position and the number of faces and cores, other sandwich construction geometries can be found: *open-face sandwich*, with one core and one face; *multi-core sandwich*, where more than two faces and one core are present. The open-face sandwich construction is almost always used as stiffened panels; readers interested in a comparison between the ordinary and multi-core sandwiches can refer to [2].

A safe design of sandwich structures requires an accurate model in order to analyze the phenomena that could occur during its service, for example buckling and failure, and to predict the static and dynamic response to external loads. For this purpose, a detailed three-dimensional FE model can be used; however, such models are computationally expensive due to the complex core geometry, especially if honeycomb or corrugated cores are modelled in detail. Thus, the approach which is generally adopted is to substitute the core with an equivalent homogenous material, i.e., a material whose mechanical behavior is equivalent, at a macroscopic level, to the behavior of the core effective medium. As a consequence, the accuracy of the solution depends on the effective prediction of the (equivalent) mechanical properties of the core.

Starting from the 1950's, many approaches have been proposed for the characterization of the equivalent materials for different core geometries, in particular the honeycomb materials. The first papers were mainly dedicated to a limited set of engineering constants [3-8], whereas only recently some theories have been proposed where the whole set of elastic constants is calculated as the result of a more general approach. For example, in [9], an energy-based approach is proposed where the strain energy of the effective core is equal to that in the equivalent medium. A review of different models and some original developments on the so-called *thickness effect* for honeycomb cores may be found in [10]. Corrugated core geometries have been also extensively studied [11]. The

substitution of the effective core with an equivalent medium leads to the assumption that all the other failure loads of the sandwich panel (i.e., the local failure modes, like the face wrinkling and the intra-cell buckling) are greater than the global mode.

Once the engineering constants of the equivalent core material are evaluated and the latter is used in place of the effective core medium, two approaches are available to predict the elasto-dynamic response of the sandwich panels, they are: three-dimensional (3D) elasticity approaches and two-dimensional (2D) models based on an a priori assumption of the through-the-thickness distribution of displacements and/or stresses (in this work we deal predominantly with displacement-based models). Among the 3D elasticity solutions, Pagano [12] solved the bending problem of rectangular, simply supported, and multilayered cross-ply plates, whereas Noor et al. [13] presented solutions for the buckling and free vibrations of simply supported sandwich panels with composite faces. Concerning 2D models, depending on the type of assumption made on the displacement field, they may be classified into two categories: the Equivalent Single Layer (ESL) and Layer-Wise (LW) models.

Within ESL models the multilayered plate is reduced to a single equivalent layer according to constitutive relations, i.e., relations between stress resultants and strain components. In the past, an attempt to apply the Classical Lamination Theory (CLT) and the First-order Shear Deformation Theory (FSDT) to the analysis of sandwich structures has been made. It is a well known fact that the CLT generally provides inaccurate results since it neglects transverse shear deformation, whereas the accuracy of the FSDT strongly depends on the shear correction factors which are needed to adjust the through-the-thickness distribution of transverse shear stresses and strains. In order to overcome the problem of the shear correction factors estimation, several higher-order theories have been formulated which account for the actual through-the-thickness distribution of transverse shear stresses and for the transverse normal deformation. Barut et al. [14] formulated a higher-order {3,2} theory based on a cubic expansion for the in-plane displacements and a quadratic variation of the transverse component. Results pertaining the static deformation of thick sandwich plates subjected to bi-sinusoidal pressure are compared with exact solutions available in literature showing favorable agreement. Kant and Swaminathan [15,16] presented the analytical formulation and some solutions for the static and natural frequency analysis of simply supported sandwich plates based on a higher-order theory which accounts for the effect of transverse shear and normal deformability and the non-linear variation across the thickness of the in-plane displacements. Later, Swaminathan et al. [17,18] applied the same higher order theory to the bending and free vibration problem of sandwich plates with anti-symmetric angle-ply face-sheets. Kheirikhah et al. [19] solved the problem of bi-axial buckling of soft-core sandwich plates using a multilayer higher order

theory: a third-order plate theory is used to model the face-sheets whereas a quadratic and a cubic expansion for the transverse and in-plane displacements are assumed, respectively, in the core. As highlighted in [20], ESL theories become inaccurate when the plate is thick, the transverse anisotropy is severe (i.e., the mechanical properties show remarkable differences from layer to layer), the materials are highly shear-deformable and exhibit high transverse normal deformability. The lack of accuracy in these conditions is caused by the use of a through-the-thickness C^1-continuous displacements field which leads to the non fulfillment of the transverse stresses continuity. Due to this, the ESL models have to be limited to the prediction of the global response quantities for relatively thin panels.

Contrary to the ESL models, in the layer-wise (LW) theories every single layer is treated as a plate itself and the kinematic description is given for every single layer. In the framework of the LW models, Rao and Desai [21] developed a higher-order mixed LW model to evaluate the natural frequencies of simply supported sandwich plates. The LW model accounts for a through-the-thickness cubic variation of the three displacement components and satisfies automatically the continuity condition of displacements and transverse stresses at the layers interfaces. Using the same kinematic assumptions of [21], Dafedar et al. [22] predicted the overall and local buckling loads of multi-core sandwich plates having an arbitrary sequence of stiff layers and cores. Moreira and Rodrigues [23] presented a LW model and applied it to the analysis of sandwich plates with thin cores. The displacement field assumed in each layer exhibits a linear variation for the in-plane components and a constant transverse displacement, thus neglecting transverse normal deformation. Although the LW models provide very accurate predictions, they are computationally expensive since the number of unknowns increases with the number of layers.

The continuity condition of displacements and transverse stresses can be satisfied a priori by assuming a displacement field with thickness-wise slope discontinuities at the interface between adjacent layers with different mechanical properties. Models based on this assumption are known as ZigZag theories (ZZ), wherein the assumed kinematics is based on an ESL-type description with the superposition of a piecewise distribution. Moreover, the ZZ models have a number of kinematic unknowns regardless of the number of layers, thus being more computationally-efficient than LW models. The ZZ theories allow global response predictions for relatively thick composite and sandwich structures that are often as accurate as those that can be achieved by the LW models. Di Sciuva, who pioneered these models, proposed a linear ZZ (LZZ) displacement-based model [24] which accounts for piecewise linear distribution across the thickness of the in-plane displacements and a priori satisfies the continuity of displacements and transverse shear stresses at interfaces (transverse normal deformability is neglected). Moreover, Di Sciuva [24] applied his LZZ model to

the linear problem of bending, free vibration and buckling load of multilayer composite plates. Later, the same author [25] formulated a ZZ plate model (CZZ) based on a piecewise cubic through-the-thickness variation for the in-plane displacements, obtained by the superposition of a linear zigzag distribution to a smeared cubic variation, and satisfying a priori the geometric and transverse shear stress continuity conditions.

The development of accurate zigzag models is motivated by the demand to perform large-scale analyses in order to reach an accurate design of high-performance composite and sandwich structures. In order to pursue this aim, the analytical form of a zigzag model has to be suitable for an efficient finite element approximation. Based on its linear and third-order ZZ models, Di Sciuva developed several finite elements [26-29]. Although numerically very efficient, C^1-continuous shape functions are required to approximate the deflection due to the presence of its second spatial derivative in the strain energy. C^0-continuos finite elements are computationally more efficient and easy to implement into FEM commercial codes. Xiaohui and Wanji [30], by using a third-order zigzag model, developed an improved C^0-continuous plate finite element and applied it to the natural frequencies problem of sandwich plates with soft cores. Pandit et al. [31,32] formulated a higher-order ZZ model where the in-plane displacements are assumed to be cubic across the thickness and the transverse displacement is constant across the face thickness and varies according to a second order polynomial through the core thickness. Based on this kinematic assumption, a C^0-continuous plate finite element model was developed and applied to the bending, vibration and buckling loads problem of soft core sandwich plates [31,32].

Recently, Tessler et al. have proposed a ZZ model for beams [33,34], plates [35-37], and shells [38] known as Refined Zigzag Theory (RZT). The kinematic field of FSDT is improved by adding a piecewise linear (across the lamina interfaces) *zigzag* function in the representation of the in-plane displacements and the transverse displacement is assumed to be constant through the thickness. The zigzag function is able to reproduce the actual in-plane displacements pattern and accounts for the shear deformation in every lamina in consistent way, thus it does not require any shear correction factor. The resulting kinematic field have a fixed number of kinematic unknowns, regardless of the number of layers, and does not enforce the continuity condition on transverse shear stresses among adjacent layers. Nevertheless, accurate predictions of all response quantities are obtained, including the transverse shear stresses that provide accurate average values at the ply-level [34,36] and improvements (with respect to the results of both LZZ and CZZ) in the through-the-thickness distributions close to clamped edges [34,36]. Moreover, Tessler et. al. [39,40] showed that within RZT, homogeneous plates should be modeled as laminated plates with infinitesimally slight levels of heterogeneity between adjacent layers. This *homogeneous limit* strategy produces highly accurate

response predictions, including those for strains and stresses, without the use of shear correction factors. The analytical form of RZT is ideally suited for developing computationally efficient C^0 finite elements. By using this benefit, both C^0 beam [41,42] and plate [43] RZT-based finite element formulations have been recently proposed.

The Refined Zigzag Theory has already been assessed on a number of elasto-static bending problems which include simply supported rectangular plates subjected to bi-sinusoidal pressure and cantilevered plates subjected to a uniform pressure [36]. The results presented for several problems have highlighted the remarkable predictive capability of the RZT and its wide range of applicability, including highly heterogeneous sandwich laminates.

The present original effort is focused on extending the original RZT formulation to vibration and buckling problems of sandwich plates. Using the RZT kinematics and non-linear von Kàrmàn strains, the plate equations of motion and related boundary conditions are derived from the D'Alembert's principle. The resulting equations are used to formulate the linear eigenvalue problems of undamped free vibration and buckling.

Symmetric and un-symmetric sandwich stacking sequences are investigated having isotropic and laminated composite face-sheets. The vibration and buckling results for sandwich plates are assessed with respect to 3D exact elasticity solutions, when available, or high-fidelity FEM solutions. If neither 3D exact elasticity solutions nor high-fidelity FEM solutions are available, results obtained with an accurate LW model are taken as reference in the comparisons. In order to assess the performances of RZT, comparisons with Di Sciuva's original zigzag theories (LZZ and CZZ) and with higher-order ESL models are also made. Moreover, a comparison with the results obtained by means of FSDT (and different values of the shear correction factors) is performed in order to assess the accuracy of this approach widely adopted in the open literature and commercial codes.

The paper is organized as follows. In the first part, the RZT displacement field is briefly presented and then, the non-linear equations of motion are derived. Subsequently, these equations are specified to the linear boundary value problem of the bending and the eigenvalue problems of undamped free vibrations and linear buckling of rectangular sandwich plates. In the final part of the paper, to test the accuracy of RZT, numerical results pertaining the bending, undamped free vibration and buckling (under uniform uni-axial, bi-axial compressive, and uniform in-plane shear load) of rectangular sandwich plates, both simply supported and clamped, are presented and compared with those resulting from the 3D exact elasticity theory, high-fidelity FE models, higher-order ESL, zigzag theories and others available in literature. For comparison purposes, the same numerical examples that appeared in several referenced papers are examined herein. The numerical

examples show that RZT ensures very accurate results, both in terms of global response quantities (deflection, natural frequencies and buckling loads) and in terms of the through-the-thickness distributions of displacements and stresses. This accuracy is maintained, without using any shear correction factor, within a wide range of variation of geometrical (span-to-thickness ratio, core-to-face thickness ratio, aspect ratio) and mechanical (face-to-core stiffness ratio) parameters of sandwich laminates. The higher-order zigzag models (CZZ) also provide correct response predictions but do not bring significant improvements in terms of accuracy with respect to linear zigzag models (RZT and LZZ), therefore corroborating the fact that the use of an higher-order approximation for the in-plane displacements is not necessary to improve the global responses prediction for sandwich plates. The FSDT is accurate in most cases if adequate shear correction factors are used; nevertheless, for thick and/or highly heterogeneous sandwich stacking sequence, this accuracy is not adequate and, as a general rule, through-the-thickness distributions of displacements and stresses exhibit significant deviations from the reference results. Even if a proper shear correction factor is used, the accuracy in estimating the natural frequencies reduces for higher-order modes. These results confirm the observation by Birman and Bert [44] on the use of shear correction factors for FSDT-based static and dynamic analysis of sandwich plates, i.e., none of the shear correction factors proposed in literature are able to produce accurate results in a wide range of cases.

2. THE REFINED ZIGZAG THEORY FOR PLATES: DISPLACEMENTS, STRAINS, AND STRESSES

Consider a laminated plate of uniform thickness *2h* with *N* perfectly bonded orthotropic layers as shown in Figure 1. The orthogonal Cartesian coordinate system (x_1, x_2, z) is taken as reference where the thickness coordinate z ranges from $-h$ to $+h$. The middle

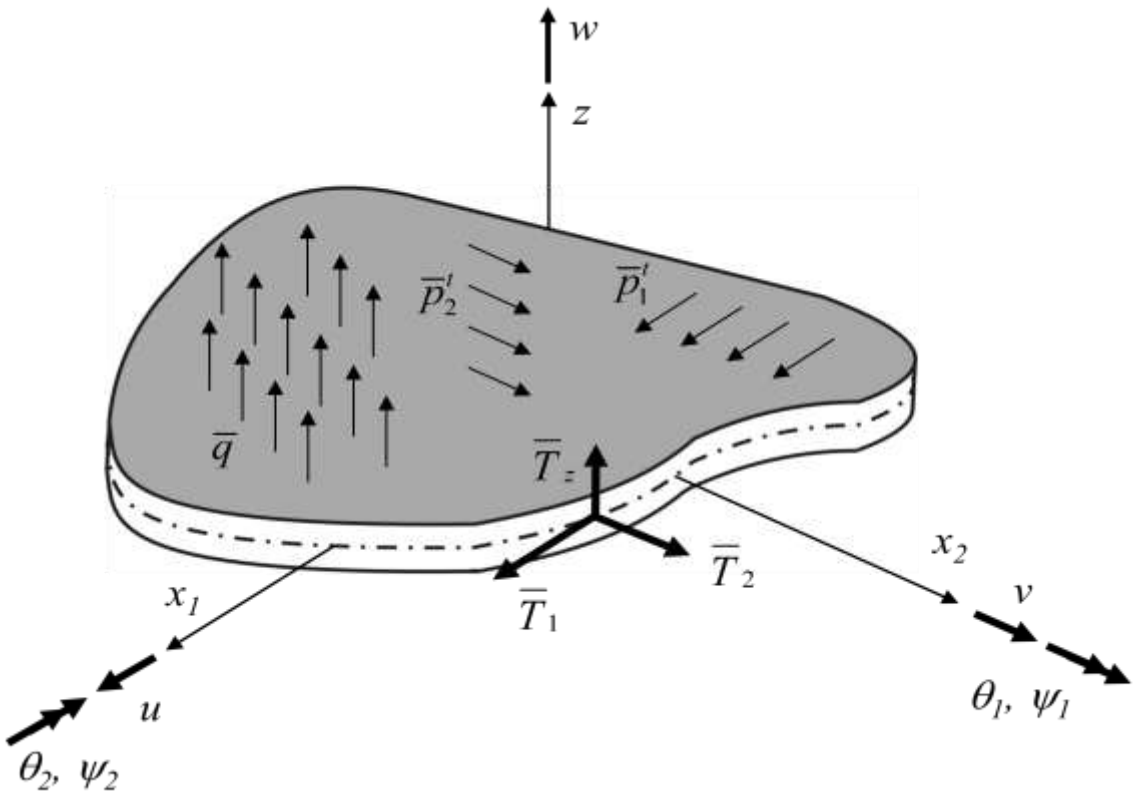

Figure 1. General plate notation.

reference plane (or midplane) of the plate, S_m, is placed on the (x_1, x_2)- plane. The plate is bounded by a cylindrical edge surface, S, constituted by two distinct surfaces, S_u and S_σ, on which the geometrical and mechanical boundary conditions are enforced, respectively. Moreover, the intersection of the surface S and of the (x_1, x_2)-plane is the curve C which represents the perimeter of the midplane, S_m. As for the edge surface, the curve C is composed by two distinct curves, C_u and C_σ, originated by the intersection of S_u and S_σ with the (x_1, x_2)-plane, respectively. Finally, S_t and S_b represent the top and bottom external surfaces of the plate (at $z= +h$ and $z= -h$), respectively.

The orthogonal components of the displacement vector, according to the kinematic assumptions of the Refined Zigzag Theory (RZT) [35,36], are expressed as

$$\begin{aligned} u_1^{(k)}(x_1, x_2, z, t) &= u(x_1, x_2, t) + z\theta_1(x_1, x_2, t) + \phi_1^{(k)}(z)\psi_1(x_1, x_2, t) \\ u_2^{(k)}(x_1, x_2, z, t) &= v(x_1, x_2, t) + z\theta_2(x_1, x_2, t) + \phi_2^{(k)}(z)\psi_2(x_1, x_2, t) \\ u_z(x_1, x_2, z, t) &= w(x_1, x_2, t) \end{aligned} \tag{1}$$

where the superscript (k) is used to denote quantities corresponding to the k^{th} lamina and t represents the time variable. The displacement field of RZT, Eq. (1), is obtained superposing the displacement field of the First-order Shear Deformation Theory (FSDT) and two *zigzag* contributions to the in-plane displacements, $\phi_\alpha^{(k)}(z)\psi_\alpha(x_1,x_2,t)\ \ (\alpha=1,2)$, which describe cross-sectional distortions that are typical of laminated composites. The kinematic unknowns of RZT are seven: the same five kinematic variables of FSDT (u and v are the in-plane uniform displacements, w is the transverse deflection, θ_1 and θ_2 are the average rotations of the transverse normal around the positive x_2-axis and the negative x_1-axis, respectively) and two additional variables (ψ_1 and ψ_2 are the amplitude of the *zigzag rotations*), see Figure 1. $\phi_1^{(k)}$ and $\phi_2^{(k)}$ are the so-called *zigzag functions*, piecewise linear functions of the thickness coordinate. The zigzag functions are independent of the state of deformation whereas depend on the thickness and of the transverse shear moduli of each layer and are set to vanish on the top and bottom laminate faces (refer to Figures 2(a) and 2 (b) which show $\phi_1^{(k)}$ and $\phi_2^{(k)}$ for a three-layered laminate)

$$\begin{aligned}&\phi_1^{(N)}(z=+h)=\phi_2^{(N)}(z=+h)=0\\&\phi_1^{(1)}(z=-h)=\phi_2^{(1)}(z=-h)=0\end{aligned}\qquad(2)$$

For the complete derivation of the zigzag functions, refer to [35,36].

In the case of homogeneous plates, the zigzag functions vanish identically and the displacement field, Eq. (1), reduces to that of FSDT. Recently, Tessler et. al. [39,40] showed that within RZT, the homogeneous plates should be modeled as laminated plates with infinitesimally small differences in the transverse shear moduli of the material layers (*homogeneous limit methodology*), thus producing highly accurate response predictions. Moreover, Gherlone [45] showed that when the external layers of a laminate are weaker than the adjacent layers, in terms of transverse shear stiffness, the RZT zigzag functions can be adapted naturally to the effective shear properties of the stacking sequence and lead to accurate results.

In order to develop a plate theory which accounts for moderately large deflection and small strains, the von Kàrmàn's non-linear strain-displacement relations are used [46]. Consistent with the displacement field of Eq. (1), the in-plane and transverse shear strains are

$$
\begin{aligned}
\varepsilon_{11}^{(k)} &= u_{,1} + z\theta_{1,1} + \phi_1^{(k)}\psi_{1,1} + \frac{1}{2}\left(w_{,1}\right)^2 \\
\varepsilon_{22}^{(k)} &= v_{,2} + z\theta_{2,2} + \phi_2^{(k)}\psi_{2,2} + \frac{1}{2}\left(w_{,2}\right)^2 \\
\gamma_{12}^{(k)} &= u_{,2} + v_{,1} + z\left(\theta_{1,2} + \theta_{2,1}\right) + \phi_1^{(k)}\psi_{1,2} + \phi_2^{(k)}\psi_{2,1} + w_{,1}w_{,2} \\
\gamma_{\alpha z}^{(k)} &= \gamma_\alpha + \beta_\alpha^{(k)}\psi_\alpha \quad (\alpha = 1,2)
\end{aligned}
\tag{3}
$$

where $(\cdot)_{,\alpha}$ denotes the partial derivative with respect to the midplane coordinate, x_α (α=1,2); moreover $\gamma_\alpha \equiv w_{,\alpha} + \theta_\alpha$ and $\beta_\alpha^{(k)} \equiv \phi_{\alpha,z}^{(k)}$ (α=1,2).

The generalized Hooke's law for the k^{th} orthotropic lamina, whose principal material directions are arbitrarily oriented with respect to the midplane reference coordinates, $(x_1, x_2) \in S_m$, is written as

$$
\begin{Bmatrix} \sigma_{11} \\ \sigma_{22} \\ \tau_{12} \\ \tau_{2z} \\ \tau_{1z} \end{Bmatrix}^{(k)} = \begin{bmatrix} C_{11} & C_{12} & C_{16} & 0 & 0 \\ C_{12} & C_{22} & C_{26} & 0 & 0 \\ C_{16} & C_{26} & C_{66} & 0 & 0 \\ 0 & 0 & 0 & Q_{22} & Q_{12} \\ 0 & 0 & 0 & Q_{12} & Q_{11} \end{bmatrix}^{(k)} \begin{Bmatrix} \varepsilon_{11} \\ \varepsilon_{22} \\ \gamma_{12} \\ \gamma_{2z} \\ \gamma_{1z} \end{Bmatrix}^{(k)}
\tag{4}
$$

where $\mathbf{C} \equiv [C_{ij}]^{(k)}$ (i,j=1,2,6) and $\mathbf{Q} = [Q_{\alpha\beta}]^{(k)}$ (α,β=1,2) are the transformed elastic stiffness coefficients referred to the (x_1, x_2, z) coordinate system and relative to the plane-stress condition that ignores the transverse-normal stress. The expression of these coefficients in terms of the elastic moduli corresponding to the material coordinates, can be found, e.g., in [47].

3. NON-LINEAR EQUATIONS OF MOTION

The plate represented in Figure 1 is subjected to a transverse pressure loading, $\bar{q}(x_1, x_2, t)$, applied on the midplane S_m, to surface tractions, $\bar{p}_1^t(x_1, x_2, t)$ and $\bar{p}_2^t(x_1, x_2, t)$, acting on the top surface, S_t, and on the bottom surface, S_b, respectively, and to traction stresses, $(\bar{T}_1, \bar{T}_2, \bar{T}_z)$, prescribed on S_σ.

The plate equations of motion and boundary conditions are derived from the D'Alembert's principle which may be written as

$$
\delta U - \delta W_i - \delta W_e = 0
\tag{5}
$$

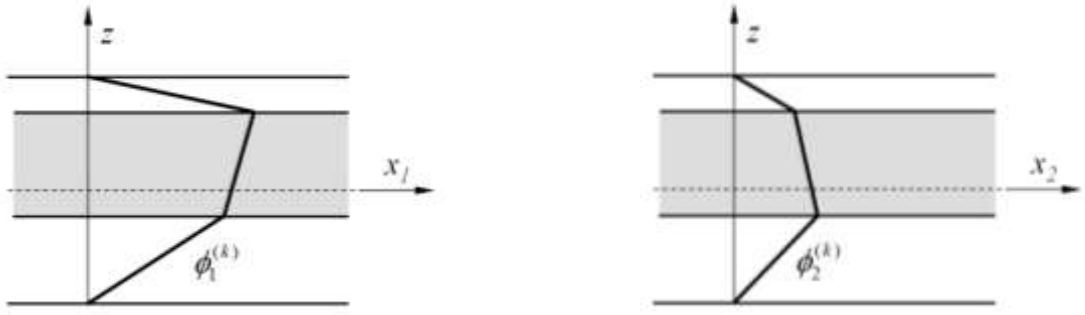

(a) Zigzag function $\phi_1^{(k)}$. (b) Zigzag function $\phi_2^{(k)}$.

Figure 2. Zigzag functions of the Refined Zigzag Theory for a three-layered laminate.

where δ is the variational operator, U, W_i and W_e represent the strain energy, the work of inertial forces and the work of the external loads, respectively.

The variation of the total strain energy, δU, is

$$\delta U \equiv \int_{S_m} \int_{-h}^{h} \left(\sigma_{11}^{(k)} \delta\varepsilon_{11}^{(k)} + \sigma_{22}^{(k)} \delta\varepsilon_{22}^{(k)} + \tau_{12}^{(k)} \delta\gamma_{12}^{(k)} + \tau_{1z}^{(k)} \delta\gamma_{1z}^{(k)} + \tau_{2z}^{(k)} \delta\gamma_{2z}^{(k)} \right) dz dS \tag{6}$$

Introducing Eqs. (1), (3) and (4) in Eq. (6) and integrating by parts, the variation of the total strain energy reads

$$\begin{aligned}
\delta U = & -\int_{S_m} \Big\{ N_{1,1}\delta u + M_{1,1}\delta\theta_1 + M_{1,1}^{\phi}\delta\psi_1 + N_{2,2}\delta v + M_{2,2}\delta\theta_2 + M_{2,2}^{\phi}\delta\psi_2 \\
& + N_{12,2}\delta u + M_{12,2}\delta\theta_1 + M_{12,2}^{\phi}\delta\psi_1 + N_{12,1}\delta v + M_{12,1}\delta\theta_2 + M_{21,1}^{\phi}\delta\psi_2 + \\
& + Q_{1,1}\delta w - Q_1\delta\theta_1 - Q_1^{\phi}\delta\psi_1 + Q_{2,2}\delta w - Q_2\delta\theta_2 - Q_2^{\phi}\delta\psi_2 + \\
& + \Big[\left(N_1 w_{,1} + N_{12} w_{,2} \right)_{,1} + \left(N_2 w_{,2} + N_{12} w_{,1} \right)_{,2} \Big] \delta w \Big\} dS + \\
& + \int_{C_\sigma} \Big\{ N_1 \delta u\ n_1 + M_1 \delta\theta_1\ n_1 + M_1^{\phi}\delta\psi_1\ n_1 + N_2\delta v\ n_2 + M_2\delta\theta_2\ n_2 + M_2^{\phi}\delta\psi_2\ n_2 + \\
& \quad N_{12}\delta u\ n_2 + M_{12}\delta\theta_1\ n_2 + M_{12}^{\phi}\delta\psi_1\ n_2 + N_{12}\delta v\ n_1 + M_{12}\delta\theta_2\ n_1 + M_{21}^{\phi}\delta\psi_2\ n_1 \\
& + \Big[Q_1 n_1 + Q_2 n_2 + N_1 w_{,1} n_1 + N_{12} w_{,2} n_1 + N_2 w_{,2} n_2 + N_{12} w_{,1} n_2 \Big] \delta w \Big\} d\Gamma
\end{aligned} \tag{7}$$

where n_1 and n_2 are the direction cosines of ***n***, the unit outward vector normal to C, with respect to the coordinates (x_1, x_2). Moreover,

$$\mathbf{N}_m^T \equiv \left(N_1, N_2, N_{12}\right) = \int_{-h}^{h} \left(\sigma_{11}^{(k)}, \sigma_{22}^{(k)}, \tau_{12}^{(k)}\right) dz \tag{8}$$

$$\mathbf{M}_b^T \equiv \left(M_1, M_1^{\phi}, M_2, M_2^{\phi}, M_{12}, M_{12}^{\phi}, M_{21}^{\phi}\right) = \int_{-h}^{h} \left(z\sigma_{11}^{(k)}, \phi_1^{(k)}\sigma_{11}^{(k)}, z\sigma_{22}^{(k)}, \phi_2^{(k)}\sigma_{22}^{(k)}, z\tau_{12}^{(k)}, \phi_1^{(k)}\tau_{12}^{(k)}, \phi_2^{(k)}\tau_{12}^{(k)}\right) dz \tag{9}$$

$$\mathbf{Q}_s^T \equiv \left(Q_2, Q_2^{\phi}, Q_1, Q_1^{\phi}\right) = \int_{-h}^{h} \left(\tau_{2z}^{(k)}, \beta_2^{(k)}\tau_{2z}^{(k)}, \tau_{1z}^{(k)}, \beta_1^{(k)}\tau_{1z}^{(k)}\right) dz \tag{10}$$

are the membrane, bending and transverse shear stress resultants, respectively.

The variation of the work of external forces, δW_e, is

$$\begin{aligned}\delta W_e \equiv & \int_{S_m} \overline{q}(x_1, x_2, t)\delta u_z dS + \int_{S_\sigma} \left(\overline{T}_1 \delta u_1^{(k)} + \overline{T}_2 \delta u_2^{(k)} + \overline{T}_z \delta u_z\right) dS + \\ & \int_{S_t} \left(\overline{p}_1^t \delta u_1^{(N)}(z = +h) + \overline{p}_2^t \delta u_2^{(N)}(z = +h)\right) dS + \\ & \int_{S_b} \left(\overline{p}_1^b \delta u_1^{(1)}(z = -h) + \overline{p}_2^b \delta u_2^{(1)}(z = -h)\right) dS\end{aligned} \tag{11}$$

Introducing Eq. (1) in Eq. (11), yields

$$\begin{aligned}\delta W_e = & \int_{S_m} \overline{q}(x_1, x_2, t)\delta w dS + \\ & \int_{C_\sigma} \int_{-h}^{h} \left[\overline{T}_1 \left(\delta u + z\delta\theta_1 + \phi_1^{(k)}\delta\psi_1\right) + \overline{T}_2 \left(\delta v + z\delta\theta_2 + \phi_2^{(k)}\delta\psi_2\right) + \overline{T}_z \delta w\right] + \\ & \int_{S_t} \left[\overline{p}_1^t \left(\delta u + h\delta\theta_1 + \phi_1^{(N)}\left(z = +h\right)\delta\psi_1\right) + \overline{p}_2^t \left(\delta v + h\delta\theta_2 + \phi_2^{(N)}\left(z = +h\right)\delta\psi_2\right)\right] dS + \\ & \int_{S_b} \left[\overline{p}_1^b \left(\delta u - h\delta\theta_1 + \phi_1^{(1)}\left(z = -h\right)\delta\psi_1\right) + \overline{p}_2^b \left(\delta v - h\delta\theta_2 + \phi_2^{(1)}\left(z = -h\right)\delta\psi_2\right)\right] dS\end{aligned} \tag{12}$$

By taking into account Eqs. (2), the equivalence among $S_m = S_t = S_b$ and introducing the following definitions

$$
\begin{aligned}
&\bar{p}_1 \equiv \bar{p}_1^t + \bar{p}_1^b \\
&\bar{p}_2 \equiv \bar{p}_2^t + \bar{p}_2^b \\
&\bar{m}_1 \equiv h\left(\bar{p}_1^t - \bar{p}_1^b\right) \\
&\bar{m}_2 \equiv h\left(\bar{p}_2^t - \bar{p}_2^b\right)
\end{aligned}
\tag{13}
$$

the variation δW_e reads

$$
\begin{aligned}
\delta W_e = &\int_{S_m} \left(\bar{p}_1 \delta u + \bar{m}_1 \delta\theta_1 + \bar{p}_2 \delta v + \bar{m}_2 \delta\theta_2 + \bar{q}(x_1, x_2)\delta w\right) dS + \\
&\int_{C_\sigma} \left[\overline{N}_{1n}\delta u + \overline{M}_{1n}\delta\theta_1 + \overline{M}^{\phi}_{1n}\delta\psi_1 + \overline{N}_{2n}\delta v + \overline{M}_{2n}\delta\theta_2 + \overline{M}^{\phi}_{2n}\delta\psi_2 + \overline{V}_{zn}\delta w\right] d\Gamma
\end{aligned}
\tag{14}
$$

where

$$
\left(\overline{N}_{1n}, \overline{M}_{1n}, \overline{M}^{\phi}_{1n}, \overline{N}_{2n}, \overline{M}_{2n}, \overline{M}^{\phi}_{2n}, \overline{V}_{zn}\right) \equiv \int_{-h}^{h} \left(\overline{T}_1, z\overline{T}_1, \phi_1^{(k)}\overline{T}_1, \overline{T}_2, z\overline{T}_2, \phi_2^{(k)}\overline{T}_2, \overline{T}_z\right) dz
\tag{15}
$$

are the force and moment resultants of the prescribed tractions.

The virtual work of the inertial forces, δW_i, is

$$
\delta W_i \equiv -\int_{S_m}\int_{-h}^{h} \rho^{(k)} \left(\ddot{u}_1^{(k)} + \ddot{\phi}_1^{(k)}\delta u_1^{(k)} + \ddot{\phi}_2^{(k)}\delta u_2^{(k)} + \ddot{u}_z\delta u_z\right) dz dS
\tag{16}
$$

where $\rho^{(k)}$ is the material mass density of the k^{th} layer. Moreover, the dot indicates differentiation with respect to the time variable, i.e., $\dot{f} \equiv \partial f / \partial t$. Substituting Eq. (1) in Eq.(16) and performing integration through the thickness, gives rise to the 2-D form of the virtual work of inertial forces

$$
\begin{aligned}
\delta W_i = -\int_{S_m} &\left[\left(I_0\ddot{u} + I_1\ddot{\theta}_1 + I_0^{\phi_1}\ddot{\psi}_1\right)\delta u + \left(I_1\ddot{u} + I_2\ddot{\theta}_1 + I_1^{\phi_1}\ddot{\psi}_1\right)\delta\theta_1 + \right. \\
&\left(I_0^{\phi_1}\ddot{u} + I_1^{\phi_1}\ddot{\theta}_1 + I_2^{\phi_1}\ddot{\psi}_1\right)\delta\psi_1 + \left(I_0\ddot{u} + I_1\ddot{\theta}_2 + I_0^{\phi_2}\ddot{\psi}_2\right)\delta v + \\
&\left.\left(I_1\ddot{u} + I_2\ddot{\theta}_2 + I_1^{\phi_2}\ddot{\psi}_2\right)\delta\theta_2 + \left(I_0^{\phi_2}\ddot{u} + I_1^{\phi_2}\ddot{\theta}_2 + I_2^{\phi_2}\ddot{\psi}_2\right)\delta\psi_2 + I_0\ddot{w}\delta w\right] dS
\end{aligned}
\tag{17}
$$

where the following definitions for the mass moments of inertia have been adopted

$$\begin{aligned}
&\left(I_0, I_1, I_2\right) \equiv \int_{-h}^{h} \rho^{(k)}\left(1, z, z^2\right) dz \\
&\left(I_0^{\phi_i}, I_1^{\phi_i}, I_2^{\phi_i}\right) \equiv \int_{-h}^{h} \rho^{(k)}\left(\phi_i^{(k)}, z\phi_i^{(k)}, \left(\phi_i^{(k)}\right)^2\right) dz
\end{aligned} \tag{18}$$

By introducing Eqs. (7), (14) and (17) in Eq. (5), by taking into account that virtual variations are arbitrary variations, the non-linear differential equations of motion are obtained

$$\delta u: \quad N_{1,1} + N_{12,2} + \bar{p}_1 = I_0 \ddot{u} + I_1 \ddot{\theta}_1 + I_0^{\phi_1} \ddot{\psi}_1 \tag{19.1}$$

$$\delta v: \quad N_{12,1} + N_{2,2} + \bar{p}_2 = I_0 \ddot{v} + I_1 \ddot{\theta}_2 + I_0^{\phi_2} \ddot{\psi}_2 \tag{19.2}$$

$$\delta w: \quad Q_{1,1} + Q_{2,2} + \left(N_1 w_{,1} + N_{12} w_{,2}\right)_{,1} + \left(N_2 w_{,2} + N_{12} w_{,1}\right)_{,2} + \bar{q} = I_0 \ddot{w} \tag{19.3}$$

$$\delta \theta_1: \quad M_{1,1} + M_{12,2} - Q_1 + \bar{m}_1 = I_1 \ddot{u} + I_2 \ddot{\theta}_1 + I_1^{\phi_1} \ddot{\psi}_1 \tag{19.4}$$

$$\delta \theta_2: \quad M_{2,2} + M_{12,1} - Q_2 + \bar{m}_2 = I_1 \ddot{v} + I_2 \ddot{\theta}_2 + I_1^{\phi_2} \ddot{\psi}_2 \tag{19.5}$$

$$\delta \psi_1: \quad M_{1,1}^{\phi} + M_{12,2}^{\phi} - Q_1^{\phi} = I_0^{\phi_1} \ddot{u} + I_1^{\phi_1} \ddot{\theta}_1 + I_2^{\phi_1} \ddot{\psi}_1 \tag{19.6}$$

$$\delta \psi_2: \quad M_{2,2}^{\phi} + M_{21,1}^{\phi} - Q_2^{\phi} = I_0^{\phi_2} \ddot{v} + I_1^{\phi_2} \ddot{\theta}_2 + I_2^{\phi_2} \ddot{\psi}_2 \tag{19.7}$$

The D'Alembert's principle also yields the variationally consistent kinematic and force boundary conditions

$$u = \bar{u} \text{ on } C_u \quad \text{or} \quad N_1 n_1 + N_{12} n_2 = \overline{N}_{1n} \text{ on } C_\sigma \tag{20.1}$$

$$v = \bar{v} \text{ on } C_u \quad \text{or} \quad N_{12} n_1 + N_2 n_2 = \overline{N}_{2n} \text{ on } C_\sigma \tag{20.2}$$

$$w = \bar{w} \text{ on } C_u \quad \text{or} \quad \mathrm{Q}_1 n_1 + \mathrm{Q}_2 n_2 + \left(N_1 w_{,1} + N_{12} w_{,2}\right) n_1 + \left(N_{12} w_{,1} + N_2 w_{,2}\right) n_2 = \overline{V}_{zn} \text{ on } C_\sigma \tag{20.3}$$

$$\theta_1 = \bar{\theta}_1 \text{ on } C_u \quad \text{or} \quad M_1 n_1 + M_{12} n_2 = \overline{M}_{1n} \text{ on } C_\sigma \tag{20.4}$$

$$\theta_2 = \bar{\theta}_2 \text{ on } C_u \quad \text{or} \quad M_{12} n_1 + M_2 n_2 = \overline{M}_{2n} \text{ on } C_\sigma \tag{20.5}$$

$$\psi_1 = \bar{\psi}_1 \text{ on } C_u \quad \text{or} \quad M_1^{\phi} n_1 + M_{12}^{\phi} n_2 = \overline{M}_{1n}^{\phi} \text{ on } C_\sigma \tag{20.6}$$

$$\psi_2 = \bar{\psi}_2 \text{ on } C_u \quad \text{or} \quad M_{21}^{\phi} n_1 + M_2^{\phi} n_2 = \overline{M}_{2n}^{\phi} \text{ on } C_\sigma \tag{20.7}$$

It is worthwhile to note that Eqs. (19) represent a generalization of the FSDT governing equations. In fact, the RZT displacement field, Eq. (1), is given by the superposition of the FSDT displacement field and of a through-the-thickness piecewise linear contribution related to the zigzag kinematic variables, ψ_1 and ψ_2. Thus, the FSDT equations of motion are Eqs. (19.1)-(19.5) where all the mass moments of inertia multiplying the second order time derivative of ψ_1 and ψ_2 are neglected. Furthermore, since the von Kàrmàn strain-displacement relations are used, the non-linear contribution appears only in the third equation: in order to recover the linear equations of motion, the contribution given by the in-plane stress resultants to this equation has to be neglected.
The plate constitutive equations are derived by substituting Eqs. (3) and (4) in Eqs. (8)-(10) and then integrating over the laminate thickness [36]

$$\begin{Bmatrix} \mathbf{N}_m \\ \mathbf{M}_b \\ \mathbf{Q}_s \end{Bmatrix} = \begin{bmatrix} \mathbf{A} & \mathbf{B} & \mathbf{0} \\ \mathbf{B}^T & \mathbf{D} & \mathbf{0} \\ \mathbf{0} & \mathbf{0} & \mathbf{G} \end{bmatrix} \begin{Bmatrix} \mathbf{e}_m^{nl} \\ \mathbf{e}_b \\ \mathbf{e}_s \end{Bmatrix} \tag{21}$$

where

$$\mathbf{e}_m^{nl} \equiv \left[u_{,1} + 1/2\left(w_{,1}\right)^2,\ v_{,2} + 1/2\left(w_{,2}\right)^2,\ u_{,2} + v_{,1} + w_{,1}w_{,2} \right]^T \tag{22.1}$$

$$\mathbf{e}_b \equiv \left[\theta_{1,1},\ \psi_{1,1},\ \theta_{2,2},\ \psi_{2,2},\ \theta_{1,2} + \theta_{2,1},\ \psi_{1,2},\ \psi_{2,1} \right]^T \tag{22.2}$$

$$\mathbf{e}_s \equiv \left[w_{,2} + \theta_2,\ \psi_2,\ w_{,1} + \theta_1,\ \psi_1 \right]^T \tag{22.3}$$

are the non-linear membrane, bending and transverse shear strain measures;

$$\mathbf{A} \equiv \int_{-h}^{h} \mathbf{C}\, dz\ ; \quad \mathbf{B} \equiv \int_{-h}^{h} \mathbf{C}\mathbf{B}_\phi\, dz\ ; \quad \mathbf{D} \equiv \int_{-h}^{h} \mathbf{B}_\phi{}^T \mathbf{C}\mathbf{B}_\phi\, dz; \quad \mathbf{G} \equiv \int_{-h}^{h} \mathbf{B}_\beta{}^T \mathbf{Q}\mathbf{B}_\beta\, dz \tag{23}$$

are the stiffness matrices and

$$\mathbf{B}_\phi \equiv \begin{bmatrix} z & \phi_1^{(k)} & 0 & 0 & 0 & 0 & 0 \\ 0 & 0 & z & \phi_2^{(k)} & 0 & 0 & 0 \\ 0 & 0 & 0 & 0 & z & \phi_1^{(k)} & \phi_2^{(k)} \end{bmatrix}; \quad \mathbf{B}_\beta \equiv \begin{bmatrix} 1 & \beta_2^{(k)} & 0 & 0 \\ 0 & 0 & 1 & \beta_1^{(k)} \end{bmatrix} \tag{24}$$

By introducing Eqs. (21) in Eqs. (19), the seven non-linear partial differential equations of motion in terms of kinematic variables are obtained.

3.1 Linear bending

In order to derive the equilibrium equations for the static linear response of the plate to external loads, the membrane strains are linearized with respect to the displacement components, see Eq. (22.1), and the inertial terms are discarded. Formally, the system of governing equations remains the same as in Eqs. (19) and the constitutive equations still read as Eqs. (21), with the only difference that the membrane strain measures are now given by $\mathbf{e}_m \equiv \left\{ u_{,1},\ v_{,2},\ u_{,2} + v_{,1} \right\}^T$. Thus, the static linear equilibrium equations read as follows

$$
\begin{aligned}
&N_{1,1} + N_{12,2} + \bar{p}_1 = 0 \\
&N_{12,1} + N_{2,2} + \bar{p}_2 = 0 \\
&Q_{1,1} + Q_{2,2} + \bar{q} = 0 \\
&M_{1,1} + M_{12,2} - Q_1 + \bar{m}_1 = 0 \\
&M_{2,2} + M_{12,1} - Q_2 + \bar{m}_2 = 0 \\
&M^{\phi}_{1,1} + M^{\phi}_{12,2} - Q^{\phi}_1 = 0 \\
&M^{\phi}_{2,2} + M^{\phi}_{21,1} - Q^{\phi}_2 = 0
\end{aligned}
\tag{25}
$$

3.2 Free vibrations

The governing equations for linear free vibrations of the plate may be obtained from Eqs. (19) by neglecting the non-linear terms of the membrane strain measures and by discarding the external loads

$$
\begin{aligned}
&N_{1,1} + N_{12,2} = I_0 \ddot{u}_1 + I_1 \ddot{\theta}_1 + I_0^{\phi_1} \ddot{\psi}_1 \\
&N_{12,1} + N_{2,2} = I_0 \ddot{v}_1 + I_1 \ddot{\theta}_2 + I_0^{\phi_2} \ddot{\psi}_2 \\
&Q_{1,1} + Q_{2,2} = I_0 \ddot{w}_1 \\
&M_{1,1} + M_{12,2} - Q_1 = I_1 \ddot{u}_1 + I_2 \ddot{\theta}_1 + I_1^{\phi_1} \ddot{\psi}_1 \\
&M_{2,2} + M_{12,1} - Q_2 = I_1 \ddot{v}_1 + I_2 \ddot{\theta}_2 + I_1^{\phi_2} \ddot{\psi}_2 \\
&M_{1,1}^{\phi} + M_{12,2}^{\phi} - Q_1^{\phi} = I_0^{\phi_1} \ddot{u}_1 + I_1^{\phi_1} \ddot{\theta}_1 + I_2^{\phi_1} \ddot{\psi}_1 \\
&M_{2,2}^{\phi} + M_{21,1}^{\phi} - Q_2^{\phi} = I_0^{\phi_2} \ddot{v}_1 + I_1^{\phi_2} \ddot{\theta}_2 + I_2^{\phi_2} \ddot{\psi}_2
\end{aligned}
\tag{26}
$$

3.3 Linear buckling

The governing equations of the linearized problem of buckling for symmetrically laminated plates subjected to uniformly distributed in-plane stress resultants, $\overline{N}_{nn}$ and $\overline{N}_{ns}$, can be formulated by using the Euler's method of the adjacent equilibrium configurations. It is assumed that the plate remains flat during the pre-buckling equilibrium state and that the external in-plane stress resultants vary neither in magnitude nor in direction during buckling [48]. Under these assumptions, the linearized stability equations reads

$$
\begin{aligned}
&N_{1,1}^{*} + N_{12,2}^{*} = 0 \\
&N_{12,1}^{*} + N_{2,2}^{*} = 0 \\
&Q_{1,1}^{*} + Q_{2,2}^{*} + N_{1,eq} w_{,11}^{*} + 2N_{12,eq} w_{,12}^{*} + N_{2,eq} w_{,22}^{*} = 0 \\
&M_{1,1}^{*} + M_{12,2}^{*} - Q_1^{*} = 0 \\
&M_{2,2}^{*} + M_{12,1}^{*} - Q_2^{*} = 0 \\
&M_{1,1}^{\phi *} + M_{12,2}^{\phi\ *} - Q_1^{\phi *} = 0 \\
&M_{2,2}^{\phi\ *} + M_{21,1}^{\phi\ *} - Q_2^{\phi *} = 0
\end{aligned}
\tag{27}
$$

with the appropriate homogenous boundary conditions. The force and moment stress resultants appearing in Eqs. (27) and denoted with $(\cdot)^{*}$, are increment with respect to the pre-buckling state, $N_{1,eq}$, $N_{2,eq}$, and $N_{12,eq}$ are the in-plane stress resultants at the equilibrium state. Moreover, since the task is only the estimation of the critical loads, non-linear terms can be neglected in the incremental stress-strain relations in order to obtain the linearized stability equations.

4. NUMERICAL RESULTS

To assess the accuracy of the Refined Zigzag Theory for the analysis of sandwich structures, the linear boundary value problem of bending and the linear eigenvalue problems of free vibration and buckling of rectangular sandwich plates, both simply supported and clamped (along one or more edges), are considered. The rectangular plates are defined in the domain $x_1 \in [0,a]$, $x_2 \in [0,b]$, $z \in [-h,h]$. Mechanical material properties of face-sheets and cores, as well as stacking sequences taken into consideration, are listed in Tables 1-3. In numerical examples, realistic core materials are used, for example the NOMEX honeycomb denoted by N (Table 2), whereas in other cases, for comparison purposes, the same mechanical properties as those reported in referenced papers are assumed.

Table 1. Mechanical properties of isotropic and orthotropic materials used for the face-sheets. The Young's moduli, $E_i^{(k)}$, and the shear moduli, $G_{ij}^{(k)}$, are expressed in GPa; the density, $\rho^{(k)}$, is expressed in kg m^{-3}.

Orthotropic Materials					Isotropic Materials			
Face material	F_1	F_2	F_3	F_4	Face material	F_5	F_6	F_7
		Ref. [30]	Ref. [49]	Ref. [30]				Ref. [50]
$E_1^{(k)}$	50	131	19	276	$E^{(k)}$	50	62.5	65.5
$E_2^{(k)}$	10	10.34	1	6.9				
$E_3^{(k)}$	10	10.34	1	6.9				
$\nu_{12}^{(k)}$	0.25	0.22	0.32	0.25	$\nu^{(k)}$	0.34	0.34	0.25
$\nu_{13}^{(k)}$	0.25	0.22	0.32	0.25				
$\nu_{23}^{(k)}$	0.25	0.49	0.49	0.3				
$G_{12}^{(k)}$	5	6.895	0.52	6.9				
$G_{13}^{(k)}$	5	6.205	0.52	6.9				
$G_{23}^{(k)}$	5	6.895	0.338	6.9				
$\rho^{(k)}$	-	1627	-	681.8				

Table 2. Mechanical properties of core materials. The Young's moduli, $E_i^{(k)}$, and the shear moduli, $G_{ij}^{(k)}$, are expressed in GPa; the mass density, $\rho^{(k)}$, is expressed in kg m^{-3}. The parameter r is the Core-to-Face Stiffness Ratio (CFSR).

Orthotropic Materials				Isotropic Materials			
Core material	N	C_1	C_2	Core material	C_3	C_4	C_5
	Ref. [53]	Ref. [49]	Ref. [30]			Ref. [30]	Ref. [50]
$E_1^{(k)}$	10^{-5}	3.2×10^{-5}	0.5776	$E^{(k)}$	62.5 r	6.89×10^{-3}	negligible
$E_2^{(k)}$	10^{-5}	2.9×10^{-5}	0.5776				
$E_3^{(k)}$	75.85×10^{-3}	0.4	0.5776				
$\nu_{12}^{(k)}$	0.01	0.99	0.0025	$\nu^{(k)}$	0.34	0	-
$\nu_{13}^{(k)}$	0.01	3×10^{-5}	0.0025				
$\nu_{23}^{(k)}$	0.01	3×10^{-5}	0.0025				
$G_{12}^{(k)}$	22.5×10^{-3}	2.4×10^{-3}	0.1079	$G^{(k)}$	-	-	0.131
$G_{13}^{(k)}$	22.5×10^{-3}	7.9×10^{-2}	0.1079				
$G_{23}^{(k)}$	22.5×10^{-3}	6.6×10^{-2}	0.22215				
$\rho^{(k)}$	-	-	1000	$\rho^{(k)}$	-	97	-

Table 3. Sandwich laminate stacking sequences (from bottom to top surface); t_c and t_f are the core and the single face-sheet thickness, respectively.

Laminate	Normalized lamina thickness, $2h^{(k)}/2h$	Lamina materials	Lamina orientation (°)	Ref.
L1	(0.05/0.05/0.8/0.05/0.05)	(F_1/ F_1/N/ F_1/ F_1)	(0/90/Core/90/0)	-
L2	($0.5t_f$/$0.5t_f$/t_c/$0.5t_f$/$0.5t_f$) refer to Sect. 4.1, 4.2	(F_2/ F_2/ C_4/ F_2/ F_2)	(0/90/Core/0/90)	[30]
L3	(0.1/0.7/0.2)	(F_6/ C_3/ F_5)	(0/Core/0)	-
L4	($0.5t_f$/$0.5t_f$/t_c/$0.5t_f$/$0.5t_f$) refer to Sect. 4.2	(F_4/ F_4/ C_2/ F_4/ F_4)	(90/0/Core/90/0)	[30]
L5	$(0.1t_f/0.1t_f)_5/t_c/(0.1t_f/0.1t_f)_5$	$(F_3/ F_3)_5/ C_1/(F_3/ F_3)_5$	$(0/90)_5$/Core/$(90/0)_5$	[49]
L6	(0.5334/4.597 /0.5334) mm	(F_7/ C_5/ F_7)	(0/Core/0)	[50]

Analytical solutions based on RZT are derived and compared with 3D exact elasticity solutions, high-fidelity finite element solutions when the former are not available, and with solutions obtained with higher-order ESL, LW or ZZ models. Moreover, a comparison with the results obtained by means of FSDT and different values of the shear correction factors is performed.

4.1 Linear bending

The numerical results presented in this section refer to the linear boundary value problem of bending of simply supported sandwich plates. Eqs. (26) have to be considered to solve the problem in the framework of RZT.

Problem 1

A simply supported, cross-ply sandwich plate subjected to a bi-sinusoidal transverse pressure, $q(x_1, x_2) = q_0 \sin(\pi x_1 / a)\sin(\pi x_2 / b)$.

For this problem, an exact elasticity solution is available (as derived by Pagano in [54]) and is used as a reference for assessing the performances of RZT. The simply supported boundary conditions read (see, Eqs.(20)),

$$x_1 = 0, a: \quad v = w = \theta_2 = \psi_2 = N_1 = M_1 = M_1^{\phi} = 0$$
$$x_2 = 0, b: \; u = w = \theta_1 = \psi_1 = N_2 = M_2 = M_2^{\phi} = 0 \tag{28}$$

and the exact solution is given by the following trigonometric expansions [36]

Table 4a. Problem 1, Laminate L1: normalized maximum (central) deflection, $\bar{w} = (10^2 D_{11} / q_0 a^4) w(a/2, b/2)$; k^2 is the shear correction factor.

			FSDT			
a/2h	Pagano	RZT	$k_x^2 = 1$ $k_y^2 = 1$	$k_x^2 = 5/6$ $k_y^2 = 5/6$	$k_x^2 = 2/3$ $k_y^2 = 2/3$	$k_x^2 = 0.0242$ $k_y^2 = 0.0225$
6	8.038	8.040	0.573	0.610	0.665	8.243
10	3.254	3.253	0.456	0.469	0.489	3.217
20	1.118	1.118	0.406	0.410	0.415	1.097
50	0.507	0.507	0.392	0.393	0.394	0.503
100	0.419	0.419	0.390	0.391	0.391	0.418

Table 4b. Problem 1, Laminate L2, core-to-face thickness ratio t_c/t_f =10: normalized maximum (central) deflection, $\bar{w} = (10^2 D_{11} / q_0 a^4) w(a/2, b/2)$; k^2 is the shear correction factor.

			FSDT			
a/2h	Pagano	RZT	$k_x^2 = 1$ $k_y^2 = 1$	$k_x^2 = 5/6$ $k_y^2 = 5/6$	$k_x^2 = 2/3$ $k_y^2 = 2/3$	$k_x^2 = 0.0030$ $k_y^2 = 0.0032$
6	58.913	58.913	0.654	0.701	0.772	76.855
10	24.702	24.702	0.504	0.521	0.546	27.936
20	6.909	6.909	0.440	0.444	0.451	7.299
50	1.478	1.478	0.422	0.423	0.424	1.520
100	0.684	0.684	0.420	0.420	0.420	0.694

$$
\begin{aligned}
w &= W \sin\left(\frac{\pi x_1}{a}\right)\sin\left(\frac{\pi x_2}{b}\right) \\
\begin{Bmatrix} u \\ \theta_1 \\ \psi_1 \end{Bmatrix} &= \begin{Bmatrix} U \\ \Theta_1 \\ \Psi_1 \end{Bmatrix} \cos\left(\frac{\pi x_1}{a}\right)\sin\left(\frac{\pi x_2}{b}\right) \\
\begin{Bmatrix} v \\ \theta_2 \\ \psi_2 \end{Bmatrix} &= \begin{Bmatrix} V \\ \Theta_2 \\ \Psi_2 \end{Bmatrix} \sin\left(\frac{\pi x_1}{a}\right)\cos\left(\frac{\pi x_2}{b}\right)
\end{aligned}
\tag{29}
$$

where $(U,V,W,\Theta_1,\Theta_2,\Psi_1,\Psi_2)$ are the unknown amplitudes of the kinematic variables which are determined from the satisfaction of the equilibrium equations, Eqs. (25). For comparison purposes, analytic solutions are also obtained using FSDT with different shear correction factors: at first, the three classical values (*1, 5/6* and *2/3*) are used for both shear correction factors k_x^2 and k_y^2, then values

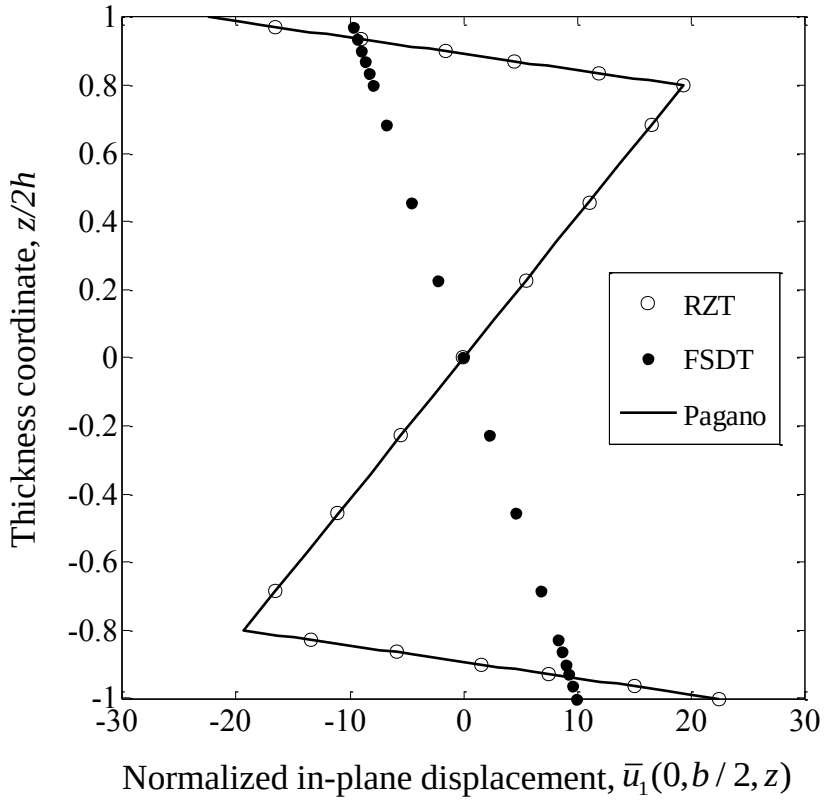

for k_x^2 and k_y^2 are estimated by means of a procedure adopted by Ferreira in [55] and based on a comparison between the shear strain energy resulting from the piecewise constant shear strain assumption, proper of FSDT, and that coming from the three-dimensional equilibrium equations.

Two square sandwich plates (laminates L1 and L2, Table 3), with laminated composite cross-ply face-sheets and a soft core, are considered and the non-dimensional transverse displacement for

different span-to-thickness ratios, *a/2h*, is compared with the exact elasticity solution and with the FSDT results (Tables 4a and 4b). Results collected in Tables 4a and 4b show that the FSDT solution,

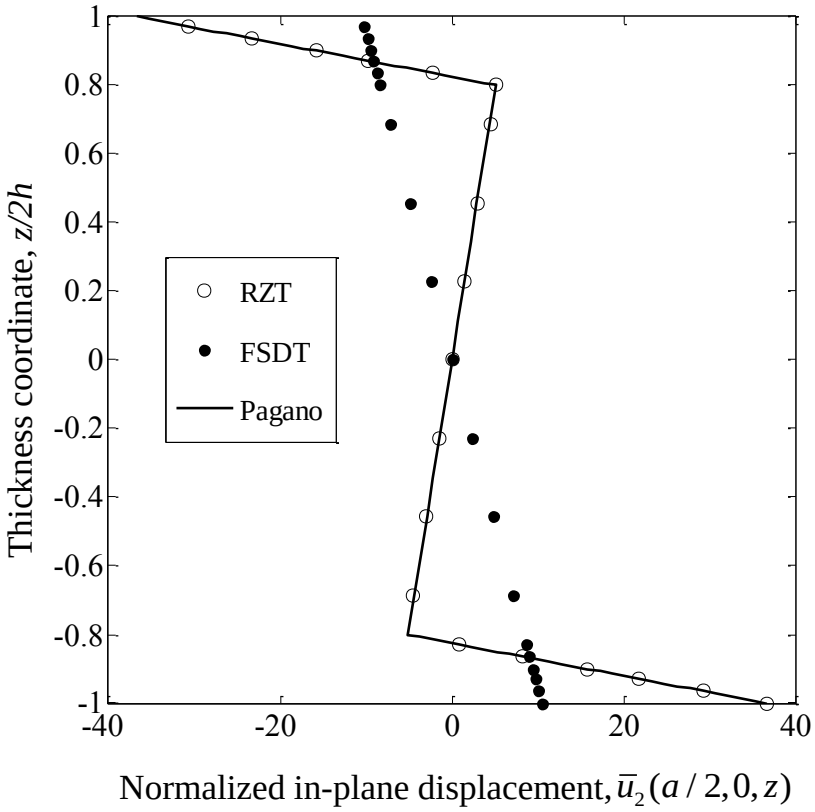

Figure 4. Problem 1, Laminate L1, *a/2h*=6: through-the-thickness distribution of normalized in-plane displacement, $\bar{u}_2 = \left(10^4 D_{11}/q_0 a^4\right) u_2^{(k)}$. The FSDT solution is obtained with $k_x^2 = k_y^2 = 0.0242$.

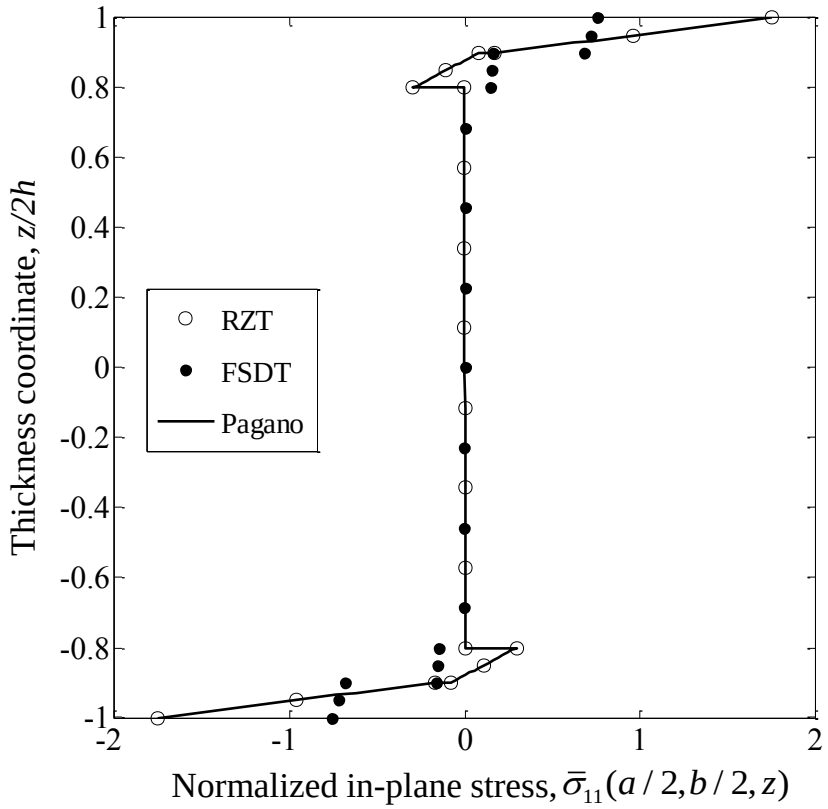

Figure 5. Problem 1, Laminate L1, *a/2h*=6: through-the-thickness distribution of normalized in-plane normal stress, $\bar{\sigma}_{11} = \left(4h^2/q_0a^2\right)\sigma_{11}^{(k)}$. The FSDT solution is obtained with $k_x^2 = k_y^2 = 0.0242$.

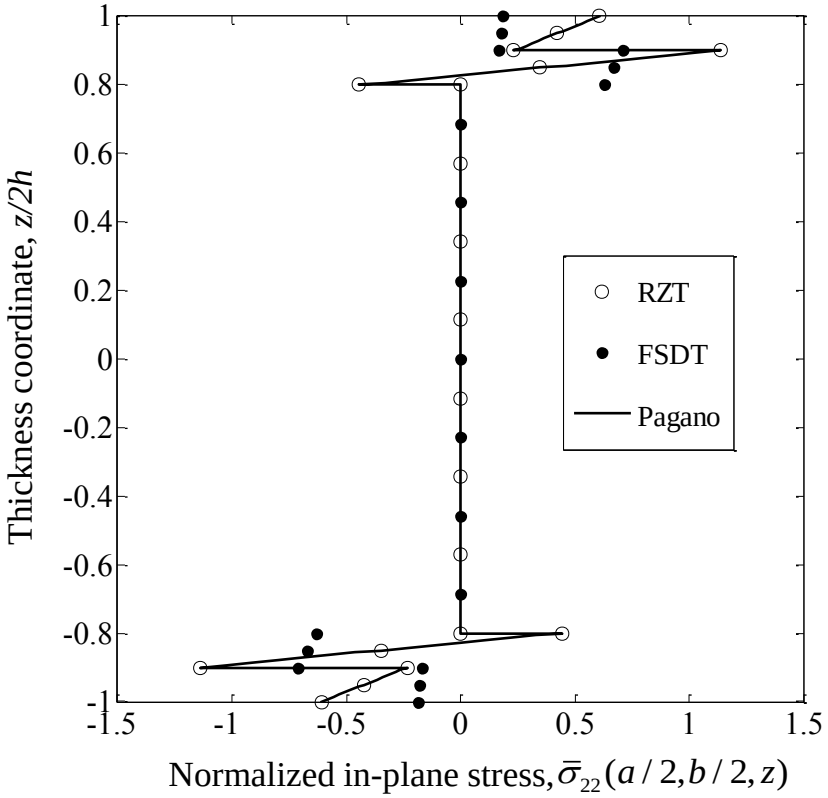

Figure 6. Problem 1, Laminate L1, *a/2h*=6: through-the-thickness distribution of normalized in-plane normal stress, $\bar{\sigma}_{22} = \left(4h^2/q_0a^2\right)\sigma_{22}^{(k)}$. The FSDT solution is obtained with $k_x^2 = ky^2 = 0.0242$.

computed with the classical values of the shear correction factors, is very stiff especially when the plate is thick, whereas the solution converges to the exact result when the span-to-thickness ratio is high (*a/2h*=100 at least). If the shear correction factors are determined by the procedure described in [55], the FSDT solution improves and it approaches the Pagano' solution, as in the case of laminate L1, also when the plate is thick (Table 4a). Nevertheless, shear correction factors computed as in [55] are not always able to produce accurate deflection predictions; see, for example, laminate L2 (Table 4b) and the related FSDT solution which is too deformable, thus leading to an overestimation of the exact solution (by 30% for *a*/2*h*=6). These results confirm the observation by Birman and Bert [44] on the use of shear correction factors for the FSDT-based static and dynamic analysis of sandwich plates, i.e., none of the shear correction factors proposed in literature are able to produce accurate results in a wide range of cases. The RZT results match very well with the 3D exact elasticity solution for every value of the span-to-thickness ratio considered and without using any shear correction factor.

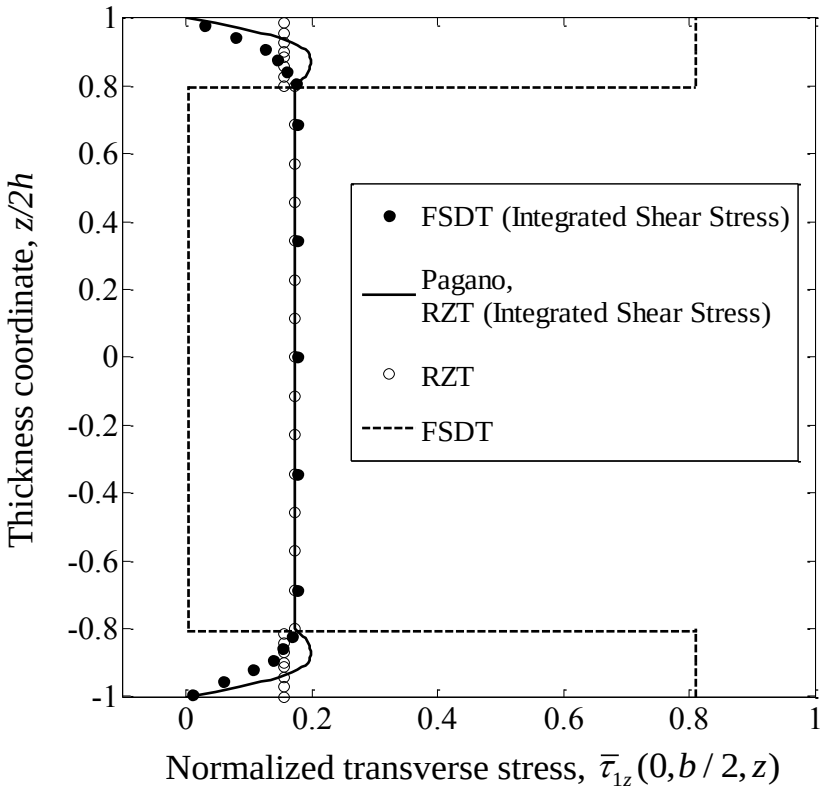

Figure 7. Problem 1, Laminate L1, *a/2h*=6: through-the-thickness distribution of normalized transverse shear stress, $\bar{\tau}_{1z} = \left(2h/q_0 a^2\right)\tau_{1z}^{(k)}$. The FSDT solution is obtained with $k_x^2 = ky^2 = 0.0242$.

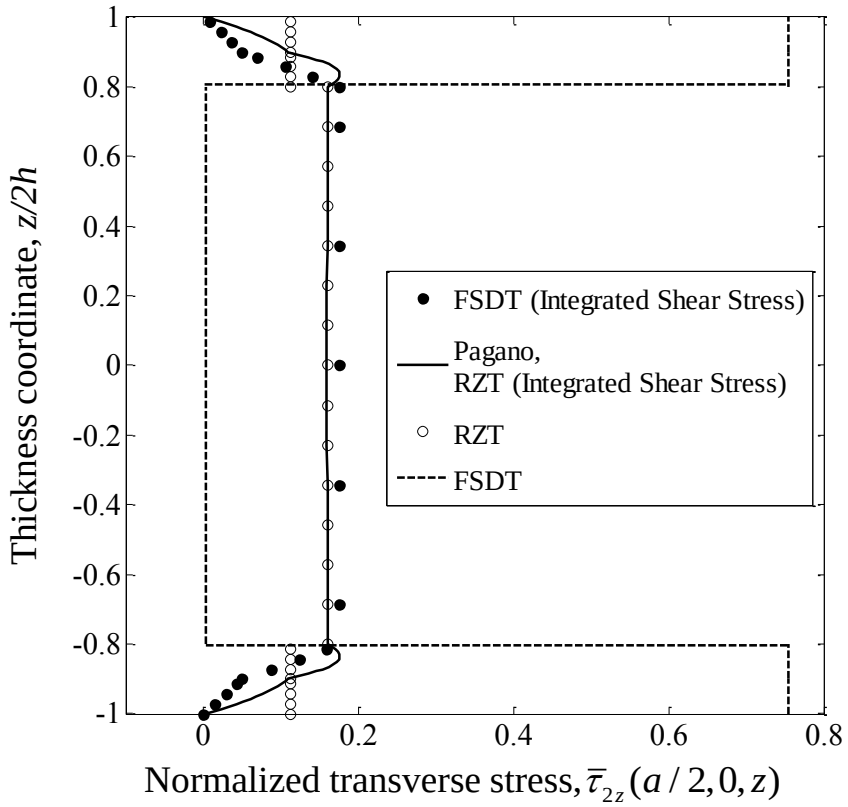

Figure 8. Problem 1, Laminate L1, *a/2h*=6: through-the-thickness distribution of normalized transverse shear stress, $\bar{\tau}_{2z} = \left(2h/q_0 a^2\right)\tau_{2z}^{(k)}$. The FSDT solution is obtained with $k_x^2 = k_y^2 = 0.0242$.

Figures 3-8 show a comparison of the through-the-thickness distribution of normalized in-plane displacements and stresses for laminate L1, with a span-to-thickness ratio *a/2h* = 6. Even if the FSDT solution obtained with suitable values of the shear correction factors [55] is accurate in terms of maximum (central) deflection, the through-the-thickness distributions of in-plane displacements and stresses are not in agreement with the reference solutions. In particular, maximum in-plane normal stresses are heavily underestimated, Figures 5 and 6. This inaccuracy represents one of the main drawbacks of the shear-correction strategy within FSDT. The RZT accurately models in-plane displacements, in-plane normal stresses and also transverse shear stresses, obtained by integration of the equilibrium equations and denoted by "*Integrated Shear Stress*" (Figures 7 and 8). The RZT transverse shear stresses obtained by the

Table 5. Problem 1, Laminate L3: comparison on normalized maximum (central) deflection, $\bar{w} = (10^2 D_{11} / q_0 a^4) w(a/2, b/2)$.

	a/2h=6	*a/2h=100*
CFSR=10^{-1}		
Pagano	1.214	0.845
RZT	1.212	0.845
FSDT		
$k_x^2 = k_y^2 = 1$	0.959	0.844
$k_x^2 = k_y^2 = 5/6$	0.982	0.844
$k_x^2 = k_y^2 = 2/3$	1.017	0.845
$k_x^2 = k_y^2 = 0.4042$	1.129	0.845
CFSR=10^{-3}		
Pagano	22.667	0.978
RZT	22.658	0.978
FSDT		
$k_x^2 = k_y^2 = 1$	0.994	0.857
$k_x^2 = k_y^2 = 5/6$	1.021	0.858
$k_x^2 = k_y^2 = 2/3$	1.062	0.858
$k_x^2 = k_y^2 = 0.0058$	24.322	0.941

constitutive equations are through-the-thickness piece-wise constant and provide an adequate esteem of the average stress in each layer.

The main physical reason for the zigzag shape of in-plane displacements relies on the different mechanical properties of adjacent layers. In order to assess the predictive capabilities of RZT with respect to this property, an important mechanical parameter of sandwich plates may be introduced, namely the Core-to-Face Stiffness Ratio, CFSR=*r*. A rectangular three-layer sandwich plate (laminate L3, Table 3) is considered: the face sheets are made using different materials, and the mechanical properties of the core are related with those of the bottom face sheet by means of the parameter *r* (see Table 2).

The non-dimensional RZT transverse displacement for different values of the span-to-thickness ratio, *a/2h*, and of CFSR=*r*, is compared with Pagano' s solution and the FSDT solution, see Table 5. Two different values of *r* are considered in order to investigate the case of a stiff core ($r=10^{-1}$) and the case of a soft core ($r=10^{-3}$). When the sandwich plate with a stiff core is considered, the use of shear corrections factors computed as in [55] lead to slightly more accurate results by

FSDT than with classical values, $k^2=1$, *5/6* and *2/3*. On the other hand, when using a soft core, the classical correction factors are inadequate whereas those based

Table 6. Problem 2, Laminate L2, core-to-face thickness ratio, t_c/t_f =10: comparison on the first six non-dimensional circular frequencies, $\bar{\omega}_{mp} = \omega_{mp}\sqrt{\left(a^4\rho_f \big/ (2h)^2 E_{2f}\right)}$, where ρ_f and E_{2f} are the mass density and the transverse Young's modulus of the face, respectively.

a/2h	Mode: *m,p*	LW [21]	RZT	LZZ	CZZ	HSDT [56]	FSDT			
							$k_x^2=1$ $k_y^2=1$	$k_x^2=5/6$ $k_y^2=$	$k_x^2=2/3$ $k_y^2=$	$k_x^2=0.00296$ $k_y^2=0.00319$
10	1,1	1.848	1.852	1.852	1.852	4.859	14.284	13.997	13.597	1.715
	1,2	3.220	3.229	3.229	3.230	8.019	32.457	31.113	29.378	2.751
	2,2	4.289	4.305	4.306	4.307	10.297	44.276	42.244	39.647	3.444
	1,3	5.224	5.241	5.243	5.244	11.738	55.138	51.95	48.057	3.910
	2,3	6.094	6.117	6.120	6.121	13.471	63.112	59.508	55.083	4.424
	3,3	7.676	7.704	7.711	7.712	16.132	77.626	72.857	67.075	5.169
100	1,1	11.940	11.946	11.946	11.946	15.509	16.277	16.273	16.266	11.843
	1,2	23.402	23.415	23.415	23.414	39.029	44.922	44.882	44.823	23.332
	2,2	30.943	30.961	30.962	30.961	54.762	64.809	64.739	64.634	30.479
	1,3	36.143	36.166	36.166	36.166	72.757	95.516	95.328	95.048	36.022
	2,3	41.447	41.474	41.475	41.474	83.441	109.56	109.35	109.02	41.008
	3,3	49.762	49.796	49.797	49.796	105.378	144.72	144.38	143.86	48.779

on [55] provide better deflection estimations (even if, for *a/2h*=6, an overestimation of more than 7% is still obtained).

Instead, RZT ensures very accurate results if compared with the reference solutions, for both cases of stiff and soft core.

4.2 Free vibrations

In this section, free-vibration analyses are conducted for simply supported and fully clamped square sandwich plates. Frequencies of undamped free vibration are the eigenvalues of Eqs. (26) and the related eigenvectors represent the corresponding modal shapes.

Problem 2

A simply supported, cross-ply square sandwich plate (Laminate L2).

Since the boundary conditions are the same as for Problem 1 and the stacking sequence is cross-ply, spatial approximations similar to those of Eqs. (29) are used to obtain the exact solution of the eigenvalue problem, Eqs. (26), in the framework of RZT

$$
\begin{aligned}
w\left(x_1,x_2,t\right) &= \sum_{m=1}^{M}\sum_{p=1}^{P} W_{mp} \sin\left(\frac{m\pi x_1}{a}\right)\sin\left(\frac{p\pi x_2}{b}\right)\sin\left(\omega_{mp}t\right) \\
\begin{Bmatrix} u\left(x_1,x_2,t\right) \\ \theta_1\left(x_1,x_2,t\right) \\ \psi_1\left(x_1,x_2,t\right) \end{Bmatrix} &= \sum_{m=1}^{M}\sum_{p=1}^{P} \begin{Bmatrix} U_{mp} \\ \Theta_{1mp} \\ \Psi_{1mp} \end{Bmatrix} \cos\left(\frac{m\pi x_1}{a}\right)\sin\left(\frac{p\pi x_2}{b}\right)\sin\left(\omega_{mp}t\right) \\
\begin{Bmatrix} v\left(x_1,x_2,t\right) \\ \theta_2\left(x_1,x_2,t\right) \\ \psi_2\left(x_1,x_2,t\right) \end{Bmatrix} &= \sum_{m=1}^{M}\sum_{p=1}^{P} \begin{Bmatrix} V_{mp} \\ \Theta_{2mp} \\ \Psi_{2mp} \end{Bmatrix} \sin\left(\frac{m\pi x_1}{a}\right)\cos\left(\frac{p\pi x_2}{b}\right)\sin\left(\omega_{mp}t\right)
\end{aligned}
\tag{30}
$$

where ω_{mp} are the circular frequencies, related to the corresponding natural frequencies, f_{mp}, by the simple relation $\omega_{mp} = 2\pi f_{mp}$ and where *m* and *p* are the number of half-waves along the x_1- and x_2-direction, respectively, of each mode shape. In Table 6, the first six non-dimensional circular frequencies obtained using RZT for two values of the span-to-thickness ratio are presented and compared with other solutions available in literature. Solution quoted as LW [21] is obtained using a layer-wise model wherein a cubic expansion in the thickness direction for the three displacement components is assumed and the continuity of transverse stresses at layer interfaces is ensured. The LW model is able to estimate accurate natural frequencies for laminated composite and sandwich plates, therefore its solution can be taken as a reference result in this comparison. Moreover, solution quoted as HSDT [56] is

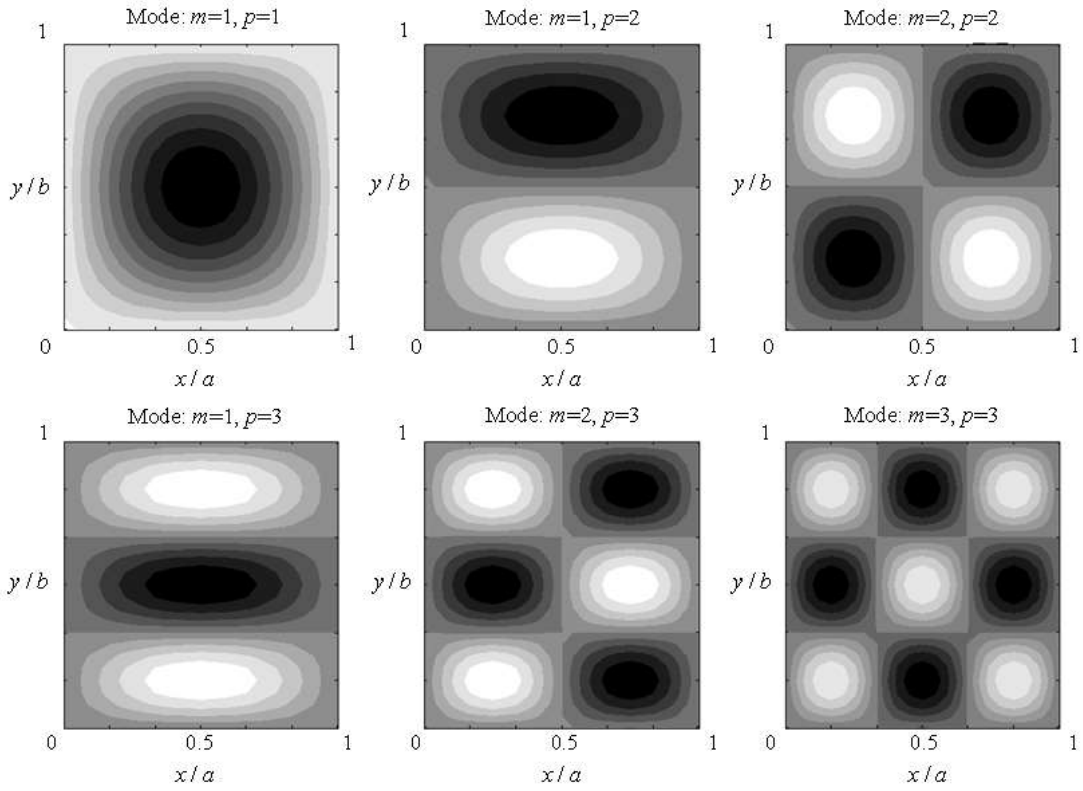

Figure 9. Problem 1, Laminate L2, *a/2h*=10: contour plots of the first six mode shapes obtained with RZT.

Table 7. Problem 2, Laminate L2, *a/2h*=10: comparison on the fundamental non-dimensional circular frequency, $\bar{\omega}_1 = \omega_1 \sqrt{\left(a^4 \rho_f / h^2 E_{2f}\right)}$, where ρ_f and E_{2f} are the mass density and the transverse Young's modulus of the face, respectively.

t_c/t_f	Exact [57]	RZT	LZZ	CZZ	HSDT [16]	FSDT (k_x^2; k_y^2)
4	1.908	1.910	1.911	1.911	8.995	1.317 *(k_x^2=0.0014;k_y^2=0.0017)*
10	1.848	1.852	1.852	1.852	4.859	1.715 *(k_x^2=0.0030;k_y^2=0.0032)*
20	2.131	2.135	2.135	2.135	3.143	2.093 *(k_x^2=0.0055;k_y^2=0.0058)*
30	2.332	2.336	2.336	2.336	2.848	2.313 *(k_x^2=0.0081;k_y^2=0.0084)*
40	2.469	2.473	2.473	2.473	2.827	2.457 *(k_x^2=0.0107;k_y^2=0.0110)*
50	2.566	2.570	2.570	2.570	2.862	2.557 *(k_x^2=0.0133;k_y^2=0.0135)*

obtained by means of a higher-order ESL theory which assumes a cubic variation across the thickness for the three displacement components. Finally, other two models are used for comparison purposes, i.e., the linear (LZZ) [24] and the cubic (CZZ) [25] Di Sciuva's original zigzag model.

Both high-order and first-order displacement-based equivalent single layer models (HSDT and FSDT with $k_x^2 = k_y^2$ = 1, 5/6, 2/3), highly overestimate the natural frequencies. This is due to the difference of mechanical properties between core and faces which causes an overestimation of the stiffness of the plate. When FSDT is used with k_x^2 and k_y^2 evaluated according to [55], although an improvement may be observed, frequencies are underestimated. The error is always below 2% when the plate is thin, *a/2h*=100, whereas ranges from 7% (fundamental frequency) to 30% (6th frequency) when the plate is moderately thick, *a/2h*=10. It is interesting that FSDT, coupled with k_x^2 and k_y^2 evaluated according to [55], ensures better results than the HSDT model. The RZT results, as well as those obtained with LZZ and CZZ, are very close to each other and compare favorably with the LW solutions, even if RZT and LZZ are linear models whereas CZZ is cubic.

Figure 9 shows the contour plots of the first six mode shapes obtained with RZT and corresponding to the frequencies reported in Table 6, for *a/2h*=10.

In order to investigate the influence of the core-to-face thickness ratio on the predictive capabilities of RZT and of other models, the fundamental frequency of laminate L2, *a*/2*h*=10, has been estimated for different values of t_c/t_f (Table 7). The exact solution for this problem, based on the propagator matrix method and on a semi-analytical solution of a higher-order mixed approach [57], is used as reference.

Also for the cases considered in Table 7, HSDT overestimates the stiffness of the plate leading to high values of the fundamental frequency. The error of HSDT reduces as the core-to-face thickness ratio increases since the plate approaches the behavior of a single-layer plate. When the core-to-face thickness ratio is small, the shear correction factors estimation procedure [55] is not effective and FSDT leads to an under-estimation of the reference frequency values (more than 30% for t_c/t_f=4*)*. For higher values of t_c/t_f, better results are obtained by means of FSDT. Taking into account the results reported in Tables 6 and 7, the shear correction factors estimation procedure [55], coupled with FSDT, provides accurate frequency estimations for thin sandwich plates or thick laminates with a large value of the core-to-face thickness ratio. The RZT confirms a very good agreement with the reference solution in the considered range of t_c/t_f, thus demonstrating the wide range of applicability of the proposed model for sandwich plates. Also the other considered linear zigzag model, LZZ, is accurate; no appreciable improvements are introduced by using a cubic zigzag model, CZZ.

Table 7. Problem 2, Laminate L2, *a/2h*=10: comparison on the fundamental non-dimensional circular frequency, $\bar{\omega}_1 = \omega_1 \sqrt{\left(a^4 \rho_f / h^2 E_{2f}\right)}$, where ρ_f and E_{2f} are the mass density and the transverse Young's modulus of the face, respectively.

t_c/t_f	Exact [57]	RZT	LZZ	CZZ	HSDT [16]	FSDT (k_x^2; k_y^2)
4	1.908	1.910	1.911	1.911	8.995	1.317 *(k_x^2=0.0014;k_y^2=0.0017)*
10	1.848	1.852	1.852	1.852	4.859	1.715 *(k_x^2=0.0030;k_y^2=0.0032)*
20	2.131	2.135	2.135	2.135	3.143	2.093 *(k_x^2=0.0055;k_y^2=0.0058)*

30	2.332	2.336	2.336	2.336	2.848	2.313 *(k_x^2=0.0081;k_y^2=0.0084)*
40	2.469	2.473	2.473	2.473	2.827	2.457 *(k_x^2=0.0107;k_y^2=0.0110)*
50	2.566	2.570	2.570	2.570	2.862	2.557 *(k_x^2=0.0133;k_y^2=0.0135)*

Problem 3

A fully clamped, cross-ply square sandwich plate (laminate L4).

Along a clamped edge all the kinematic variables vanish. For clamped boundary conditions, the RZT exact solution does not

Table 8. Problem 3, Laminate L4, core-to-face thickness ratio, t_c/t_f=8: comparison on the first ten non-dimensional circular frequencies, $\bar{\omega}_{mp} = 100\omega_{mp} a\sqrt{\left(\rho_c / E_{1f}\right)}$, where ρ_c is the mass density of the core and E_{1f} is the longitudinal Young's modulus of the face.

a/2h	Mode: *m,p*	3D FE [58]	$RZT_{(M=P=10)}$	$LZZ_{(M=P=10)}$	$CZZ_{(M=P=10)}$	$FSDT_{(M=P=10)}$ k_x^2=0.0834; k_y^2=0.1445
5	1,1	12.046	12.327	12.391	12.403	11.434
	2,1	18.270	18.158	18.263	18.292	16.407
	1,2	20.572	21.543	21.673	21.711	19.562
	2,2	24.874	25.474	25.637	25.687	22.429
	3,1	26.405	26.092	26.313	26.379	22.850
	3,2	30.644	31.787	32.053	32.136	27.505
	1,3	-	32.279	32.520	32.611	28.511
	2,3	-	35.164	35.436	35.538	28.812
	4,1	-	35.696	36.182	36.307	30.856
	3,3	-	40.164	40.535	40.723	32.929
10	1,1	11.224	11.444	11.479	11.477	11.183
	2,1	16.678	16.456	16.502	16.504	16.094
	1,2	18.965	19.813	19.883	19.883	19.055

3,1	22.710	22.917	22.977	22.983	22.199
2,2	23.527	23.160	23.248	23.253	22.356
3,2	28.073	28.194	28.295	28.303	27.113
1,3	-	29.521	29.63	29.639	28.120
4,1	-	30.120	30.219	30.243	28.797
2,3	-	31.898	32.014	32.020	30.449
4,2	-	34.386	34.548	34.620	32.766

exist and an approximate solution has been developed by means of the Rayleigh-Ritz method. The kinematic variables are approximated in the following way

$$\left(u,v,w,\theta_1,\theta_2,\psi_1,\psi_2\right)=\sum_{m=1}^{M}\sum_{p=1}^{P}\left(U_{mp},V_{mp},W_{mp},\Theta_{1mp},\Theta_{2mp},\Psi_{1mp},\Psi_{2mp}\right)\chi_m(x_1)\chi_p(x_2) \tag{31}$$

where $\chi_m(x_1)$ and $\chi_p(x_2)$ are Gram-Schmidt polynomials built to satisfy the geometric boundary conditions; for the particular expressions of $\chi_m(x_1)$ and $\chi_p(x_2)$, see Ref. [35]. In Table 8, the first ten circular frequencies, computed with different approaches, are compared with the RZT results. Solution cited as 3D FE [58] is obtained by means of three-dimensional finite element analysis and it can be considered as a reference result. For comparison purposes, solutions are also obtained with FSDT (shear correction factors as in [55]). Moreover, Di Sciuva's linear (LZZ) and cubic (CZZ) models are involved in the comparison. Also the FSDT, LZZ and CZZ solutions are obtained by means of the Rayleigh-Ritz's method using a similar procedure established for RZT (see Eq. (31)). Pursuant to a convergence analysis performed for the RZT, LZZ, CZZ, and FSDT solutions, ten Gram-Schmidt polynomials in both directions, i.e. M=P=10, are found to be the minimum number able to guarantee convergent results.

As for Problem 2, FSDT under-estimates the reference frequency values, especially for higher-order modes (error up to 11 %). The error reduces by increasing the span-to-thickness ratio and the results approach those of the 3D FEM solutions. From the results reported in Table 8, RZT, LZZ and CZZ appear accurate in an engineering sense, if compared with the reference solution. The RZT

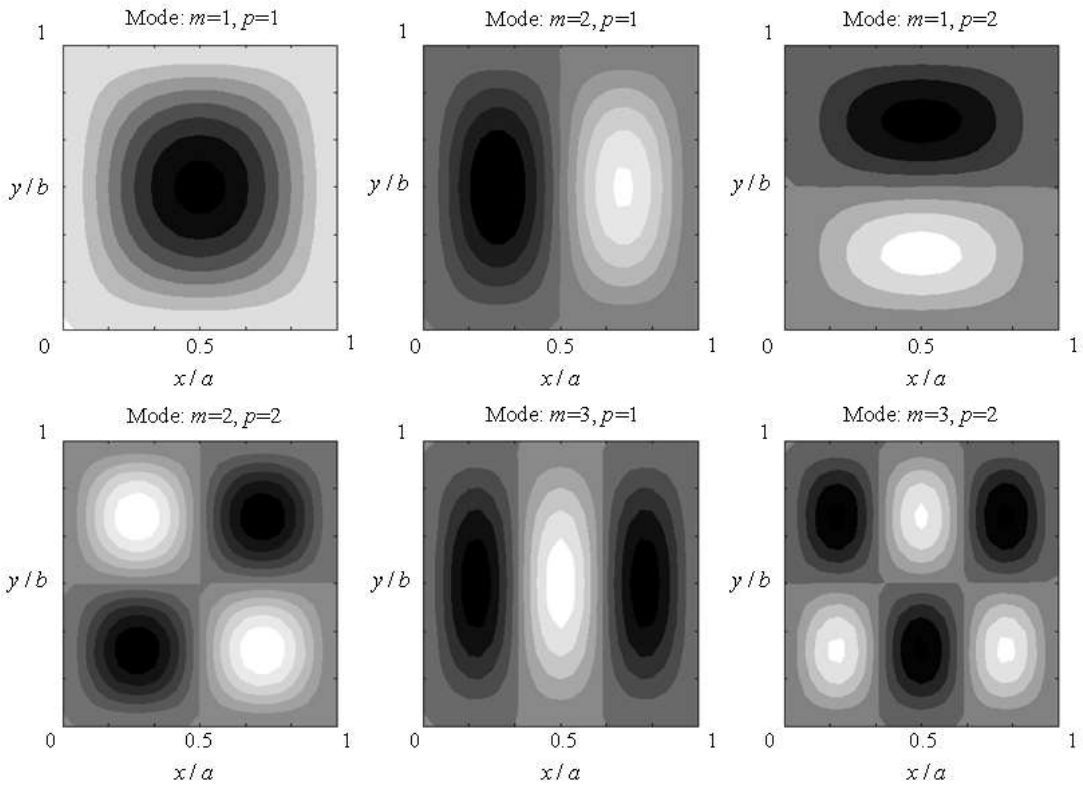

Figure 10. Problem 3, Laminate L4, *a/2h*=5: contour plots of the first six mode shapes obtained with RZT.

Table 9. Problem 4, Laminate L5: comparison of uni-axial overall buckling load parameter, $\bar{n}_1 = \bar{N}_1^{cr} b^2 / \left(E_{2f} h^3 \right)$ where $\bar{N}_1^{cr}$ is the uniform uni-axial critical load and E_{2f} is the transverse Young's modulus of the face.

	$t_f/2h$ =0.025			$t_f/2h$ =0.05			$t_f/2h$ =0.1		
a/2h	*5*	*10*	*20*	*5*	*10*	*20*	*5*	*10*	*20*
3D [13]	1.503	2.238	2.554	2.082	3.737	4.659	2.605	5.608	7.897
RZT	1.539	2.263	2.566	2.115	3.765	4.681	2.628	5.633	7.921
LZZ	1.540	2.264	2.566	2.120	3.769	4.683	2.642	5.652	7.931
CZZ	1.572	2.281	2.571	2.139	3.784	4.688	2.632	5.637	7.923
FSDT									
$k_x^2 = k_y^2 = 1$	1.682	2.337	2.589	2.622	4.122	4.811	4.029	6.952	8.491
$k_x^2 = k_y^2 = 5/6$	1.566	2.278	2.571	2.390	3.971	4.758	3.623	6.631	8.368

$k_x^2=k_y^2=2/3$	1.418	2.195	2.543	2.110	3.763	4.681	3.147	6.202	8.189
k_x^2, k_y^2	1.539	2.263	2.566	2.116	3.767	4.682	2.620	5.638	7.926
	$(k_x^2=0.820, k_y^2=0.782)$			$(k_x^2=0.697, k_y^2=0.643)$			$(k_x^2=0.541, k_y^2=0.479)$		

preserves its remarkable accuracy also for clamped boundary condition, even considering higher modes, thus ensuring a wide range of applicability of this model. Results reported in Table 8 put also in evidence two points. Firstly, the LZZ and CZZ capabilities in predicting accurate natural frequencies are not affected by the clamped boundary conditions, contrary to what happens to transverse shear stresses estimation near clamped edges [33-36]. Secondly, as already highlighted by Di Sciuva and Icardi [59], the use of an higher-order zigzag model does not ensure improvement in the prediction of the global responses, above all in the range of core-to-face thickness ratio considered in the present numerical cases.

From these observations, we can state that a relevant improvement in the prediction capability of global response of an ESL theory is due to the use of a suitable zigzag function more than to the adoption of higher-order polynomial expansions.

The contour plots of the first six mode shapes, obtained with RZT for $a/2h$=5, are represented in Figure 10.

4.3 Linear buckling

In this section, results concerning the critical buckling load of (i) simply supported sandwich plates subjected to uniform uni-axial compressive load, (ii) fully clamped sandwich plates under uniform bi-axial compressive load, and (iii) plates supported on two edges, clamped on the others and subjected to in-plane shear load, are presented. Buckling loads may be calculated within RZT as eigenvalues of the stability equations, Eqs. (27), coupled with suitable homogeneous boundary conditions. The generalized displacement components in Eqs. (27) are measured from the state just prior to the occurrence of the buckling.

Problem 4

A square sandwich plate (laminate L5), simply supported on all edges and subjected to a uniform uni-axial compressive load, $\bar{N}_1$.

Since the boundary conditions are of simple support and cross-ply sandwich plates are considered, the spatial approximation of the unknown kinematic variables are given by expressions similar to

those of Eqs. (30). Comparison of the buckling critical load, for different values of span-to-thickness ratio, *a/2h*, and face-to-overall thickness ratio, $t_f/2h$, is made. Several models are considered in order to assess the predictive capabilities of RZT (see Table 9). Solution quoted as 3D [13] is taken as reference in the comparison: the face-sheets and the core are treated as three dimensional continua and the buckling response is obtained by using the solution procedure suggested by Srinivas and Rao [56].

The FSDT, with the classical shear correction factors, over-estimates the uni-axial buckling load parameter; whereas the results converge to the reference solutions if the procedure proposed in [55] is adopted to calculate k_x^2 and k_y^2. For the present problem, FSDT provides accurate results since, as it has been highlighted in the previous section, the shear correction factors estimation procedure [55] is effective when the plate has a thick core layer, regardless the span-to-thickness ratio. The LZZ and CZZ results are very close to those obtained by means of RZT, the latter being slightly better and leading to highly accurate predictions within the considered ranges of span-to-thickness ratio, *a/2h*, and face-to-overall thickness ratio, $t_f/2h$.

Problem 5

A fully clamped rectangular sandwich plate (laminate L6) under bi-axial compression ($\bar{N}_2 = 0.5\bar{N}_1$).

The same problem has been solved in [50] and, for comparison purpose, the same material and geometrical configuration has been used here. The RZT approximate solution is obtained by using the Rayleigh-Ritz method as for the dynamic Problem 2, Sect. 4.2, and the same spatial approximation for the incremental kinematic variables as in Eqs. (31). The FSDT, LZZ and CZZ solutions are computed in a similar manner. Since the RZT, LZZ, CZZ and FSDT solutions are approximate, a convergence study was carried out to select the required number of Gram-Schmidt polynomials, i.e. the values of M and P. The critical buckling stress, for different values of the aspect ratio *a/b*, is estimated by means of the above mentioned models and compared with several other solutions available in literature. In particular, two references are considered: a 2D finite element solution, by Khatua and Cheung [51], and one obtained with the Finite Strip Method (FSM), by Yuan and Dawe [52], wherein the core is represented as a three-dimensional solid with quadratic through-the-thickness in-plane displacements and a linear transverse displacement, whereas the face-sheets are modeled as thin plates, i.e. according to the assumptions of the CLT.

In Table 10, the critical buckling stresses are compared for the four above stated formulations and the results reported in [50].

The FSDT results, obtained with the classical values for the shear correction factors, overestimate

the reference solutions available in literature especially for values of the aspect ratio, *a*/*b*, lower than 1. Instead, the use of the shear correction factors computed as in [55] improves FSDT critical buckling stress predictions. Solutions obtained with the Di Sciuva's linear (LZZ) and cubic (CZZ) zigzag models fit very well, in an engineering sense, with those obtained with the RZT, for every value of the aspect ratio considered. Comparisons made in Table 10 show that RZT is able to predict the critical buckling stresses that are in close agreement with the reference solutions [50]. These results also confirm that the use of a higher order model does not lead to relevant improvements in terms of global response predictions. It is worth remarking that as in the free vibration analyses (Problem 2, Sect. 4.2), the LZZ and CZZ deficiencies near the clamped edge do not affect the capability of these models to predict the critical buckling loads accurately.

Problem 6

A rectangular sandwich plate (laminate 7), simply supported on two opposite edges and clamped along the other edges, subjected to a uniform in-plane shear load, $\bar{N}_{12}$.

The same problem has been solved in [50], therefore, for comparison purposes, the same material properties and geometry have been used here. The RZT approximate solution is obtained by using the Rayleigh-Ritz method. In this case, the boundary conditions read as:

Table 10. Problem 5, Laminate L6, *b*=0.5969 m: comparison of the critical buckling stress ($\bar{\sigma}_{cr} = \bar{N}_1^{cr} / 2t_f$ in N mm^{-2}.)

	Aspect ratio (*a*/*b*)		
	0.5	0.7	1.0
Khatua and Cheung [51]	170.91	112.41	81.45
Yuan and Dawe [52]	170.11	111.15	80.95
RZT $_{(M=P=8)}$	170.37	111.25	80.99
LZZ$_{(M=P=7)}$	170.39	111.28	81.01
CZZ$_{(M=P=4)}$	170.65	111.54	81.25
FSDT$_{(M=P=6)}$			
$k_x^2 = k_y^2 = 1$	220.72	129.73	89.65
$k_x^2 = k_y^2 = 5/6$	220.36	129.61	89.59
$k_x^2 = k_y^2 = 2/3$	219.81	129.43	89.51
$k_x^2 = k_y^2 = 0.0264$	170.26	111.18	80.93

Table 11. Problem 6, Laminate L6, b=0.5969 m: comparison of the critical buckling stress ($\bar{\sigma}_{cr} = \bar{N}_{12}^{cr} / 2t_f$ in N mm^{-2}).

	Aspect ratio (a/b)		
	0.5	0.7	1.0
Yuan and Dawe [52]	256.80	172.00	134.60
$RZT_{(M=P=9)}$	257.44	172.04	134.54
$LZZ_{(M=P=12)}$	256.98	171.78	134.29
$CZZ_{(M=P=5)}$	258.17	173.28	135.63
$FSDT_{(M=P=10)}$			
$k_x^2 = k_y^2 = 1$	336.59	208.81	158.12
$k_x^2 = k_y^2 = 5/6$	336.00	208.54	157.95
$k_x^2 = k_y^2 = 2/3$	335.10	208.14	157.69
$k_x^2 = k_y^2 = 0.0264$	256.68	171.44	133.96

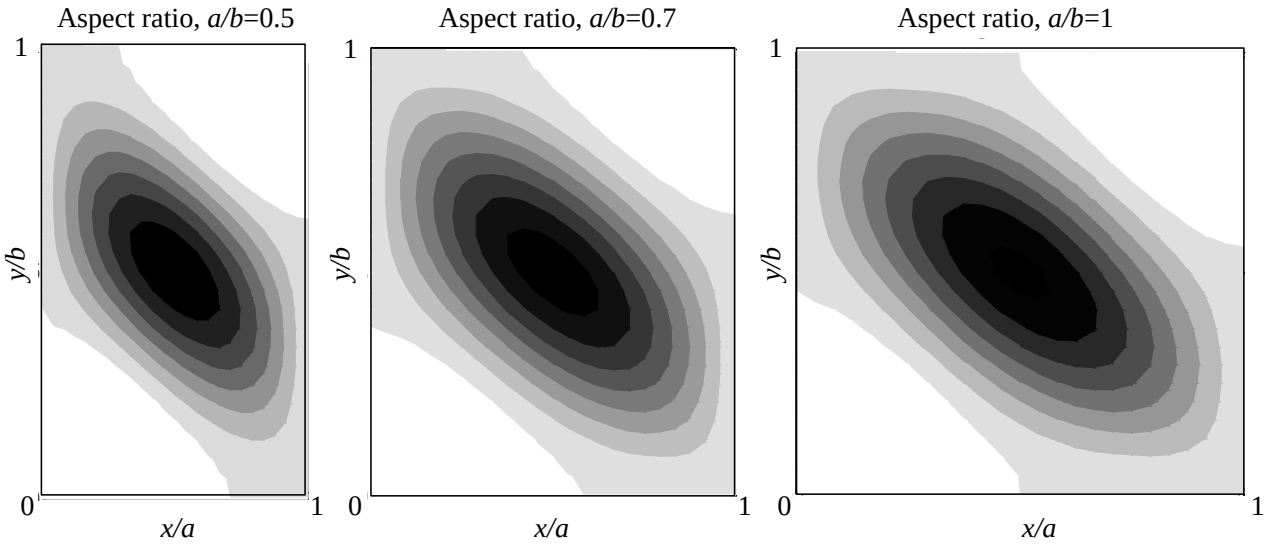

Figure 11. Problem 6, Laminate L6: contour plots of the buckling mode shapes obtained with RZT for each values of the aspect ratio considered in Table 11.

$$
\begin{aligned}
&x_1 = 0, a: \;\; v^* = w^* = \theta_2^* = \psi_2^* = N_1^* = M_1^* = M_1^{\phi *} = 0 \\
&x_2 = 0, b: \; u^* = v^* = w^* = \theta_1^* = \theta_2^* = \psi_1^* = \psi_2^* = 0
\end{aligned}
\tag{32}
$$

where the displacements and stress resultants denoted with $(g)^*$ are incremental with respect to the pre-buckling state. The incremental kinematic variables are approximated in the following way

$$\left(u^*, v^*, w^*, \theta_1^*, \theta_2^*, \psi_1^*, \psi_2^*\right) = \sum_{m=1}^{M}\sum_{p=1}^{P}\left(U_{mp}, V_{mp}, W_{mp}, \Theta_{1mp}, \Theta_{2mp}, \Psi_{1mp}, \Psi_{2mp}\right)\chi_m(x_1)\chi_p(x_2) \tag{33}$$

where $\chi_m(x_1)$ and $\chi_p(x_2)$ are trigonometric functions and Gram-Schmidt polynomials, respectively, built to satisfy the geometric boundary conditions.

In a similar way, the FSDT, LZZ and CZZ solutions are obtained by means of the Rayleigh-Ritz' method.

Critical buckling stress values obtained by means of several models and with different values of the aspect ratio *a/b*, are reported in Table 11. Also in this case, the FSDT solution obtained with the classical values of the shear correction factors, overestimates the solution available in literature [52] and the others reported for comparison. When the shear correction factors are computed by means of the procedure suggested in [55], FSDT improves and its results approach the reference solutions, even if the solution remains conservative for every value of the aspect ratio considered. The use of a higher-order model, i.e. the Di Sciuva's cubic zigzag model (CZZ), leads to a slightly higher values of the critical buckling stress if compared with those of the linear model (LZZ). It is demonstrated, also in this case, that the results computed by means of LZZ and CZZ are not negatively affected by the presence of clamped boundary conditions. The models are in fact able to estimate critical buckling stresses that are in good agreement with the reference solutions. Critical buckling stresses obtained with RZT compare favorably with the reference values within the considered range of aspect ratio values.

Table 11 collects the RZT, LZZ, CZZ and FSDT convergent results obtained with M and P numbers of Gram-Schmidt polynomials that are reported as subscript in Table 11.

The contour plots of the buckling mode, obtained with RZT for each values of the aspect ratio considered in Table 11, are represented in Figure 11.

Results of Tables 9-11 show that RZT provides accurate predictions of critical buckling loads in several load and boundary conditions, thus demonstrating the wide range of applicability of the proposed model.

Conclusions

The Refined Zigzag Theory (RZT) has been used in this paper in order to obtain the non-linear (in the von Kàrmàn sense) equations of motion and related boundary conditions of laminated composite and sandwich plates. The governing equations have been derived and used to solve the (i) linear boundary value problem of bending and, for the first time, the linear eigenvalue problems of (ii) undamped free vibrations and (iii) buckling under uni- and bi-axial compression and shear load of sandwich plates, both simply supported and clamped. For the simply supported plates, the exact solution has been obtained by means of the usual trigonometric expansions of the kinematic unknowns, whereas, for the case of clamped boundary conditions, approximate solutions have been obtained by means of the Rayleigh-Ritz method.

Several numerical studies have been performed in order to assess the accuracy of RZT in predicting global response quantities for sandwich plates, i.e., maximum deflection, natural frequencies, and buckling loads, and in evaluating local response quantities, i.e., through-the-thickness distributions of displacements and stresses. Moreover, the influence of several geometrical (span-to-thickness ratio, core-to-face thickness ratio, aspect ratio) and mechanical (core-to-face stiffness ratio) parameters as well as of boundary conditions, has been investigated.

In addition, for comparison purposes, results obtained with several previously developed linear and cubic zigzag models (LZZ and CZZ), 3D exact elasticity solutions, and high-fidelity finite element solutions have been presented. An investigation on the performance of the First-order Shear Deformation Theory (FSDT) with different shear correction factors has also been performed.

The numerical studies have demonstrated that for the sandwich plates examined, RZT exhibits the same accuracy in predicting the global response quantities as the LZZ and CZZ theories. No significant improvements are brought by the use of a higher-order zigzag model (CZZ) as compared to the linear theories (RZT and LZZ). This observation confirms the importance of enriching the model kinematic description by means of a zigzag function rather than increasing the order of the approximation for the in-plane displacement components. The RZT preserves its accuracy changing the sandwich geometrical or mechanical parameters, the boundary and the loading conditions, thus ensuring a wide range of applicability. Moreover, RZT does not require any shear correction factor to provide good predictions.

Furthermore, the present numerical studies have also demonstrated that FSDT, using specially derived shear correction factors, gives more accurate predictions for the global response quantities than those obtained with the classically adopted values of k_x^2 and k_y^2. In the majority of cases, the shear correction factors estimated by means of a procedure based on a transverse shear strain energy equivalence ensures accurate prediction of the maximum deflections, fundamental frequencies and

overall critical buckling loads. Nevertheless, the accuracy decreases when the sandwich plate is thick or it has a low value of the core-to-face stiffness ratio or core-to-face-thickness ratio. In particular, for decreasing values of the core-to-face stiffness ratio, an over-estimation of the maximum deflection, as well as an under-estimation of the natural frequencies and overall critical buckling loads, are observed. Moreover, in the free vibration problem, the under-estimation is stronger for the higher-order modes but, for a certain mode, the increase in the span-to-thickness ratio leads to more accurate results. Even when FSDT, coupled with more accurate shear correction factors, provides accurate esteems of the maximum deflection, the through-the-thickness distributions for in-plane displacements and stresses are quite far from the reference stresses, in particular resulting in a under-estimation of the maximum stresses.

The RZT is accurate not only for static analyses of sandwich plates, as demonstrated in a number of previous papers, but also for estimating natural frequencies and buckling loads, as revealed by the numerical results of the present paper. By virtue of its accuracy, computational efficiency, and ease of implementation into FEM codes (requiring C^0-continuous kinematic variables), the RZT-based finite elements appear to be highly desirable for a wide range of laminated composite and sandwich structural analyses.

References

[1] Noor AK, Burton CW. Computational models for sandwich panels and shells. Applied Mechanics Review 1996; 49(3): 155-199.

[2] Weeks CA, Sun CT. Multi-core composite laminates. Journal of Advanced Materials 1994; 25(3): 28-37.

[3] Chang CC, Ebcioglu IK. Effect of cell geometry on the shear modulus and on density of sandwich panel cores. Journal of Basic Engineering 1961; 83(4): 513-518.

[4] Penzien J, Didriksson T. Effective shear modulus of honeycomb cellular structure. AIAA Journal 1964; 2(3): 531-535.

[5] Masters IG, Evans KE. Models for the elastic deformation of honeycombs. Composite Structures 1996; 35(4): 403-422.

[6] Becker W. The in-plane stiffnesses of a honeycomb core including the thickness effect. Archive of Applied Mechanics 1998; 68: 334-341.

[7] Becker W. Closed-form analysis of the thickness effect of regular honeycomb core material. Composite Structures 2000; 48: 67-70.

[8] Grediac M. A finite element study of the transverse shear in honeycomb cores. International Journal of Solids and Structures 1993; 30(13): 1777-1788.
[9] Hole J, Becker W. A refined analysis of the effective elasticity tensor for general cellular sandwich cores. International Journal of Solids and Structures 2001; 38(21): 3689-3717.
[10] Gherlone M, Di Sciuva M. Analytical models for the homogenization of sandwich honeycomb cores. In: Proceedings of 17th Congresso Nazionale AIDAA, Rome, 2003, pp. 457-466.
[11] Ko W.L. Elastic constants for sf/db corrugated sandwich cores. NASA Technical Paper n° 1562, 1980.
[12] Pagano NJ. Exact solutions for rectangular bidirectional composites and sandwich plates. Journal of Composite Materials 1970; 4(1): 20-34.
[13] Noor AK, Peters JM, Burton WS. Three-dimensional solutions for initially stressed structural sandwiches. Journal of Engineering Mechanics 1994; 120(2): 284-303.
[14] Barut A, Madenci E, Heinrich J, Tessler A. Analysis of thick sandwich construction by a {3,2}-order theory. International Journal of Solids and Structures 2001; 38(34): 6063-6077.
[15] Kant T, Swaminathan K. Analytical solutions for the static analysis of laminated composite and sandwich plates based on an higher order refined theory. Composite Structures 2002; 56(4): 329-334.
[16] Kant T, Swaminathan K. Analytical solutions for free vibration of laminated composite and sandwich plates based on higher-order theory. Composite Structures 2001; 53(1): 73-85.
[17] Swaminathan K, Patil SS, Nataraja MS, Mahabaleswara KS. Bending of sandwich plates with antisymmetric angle-ply face-sheets- analytical evaluation of higher order refined computational models. Composite Structures 2006; 75(1-4): 114-120.
[18] Swaminathan K, Patil SS. Analytical solutions using a higher order refined computational model with 12 degree of freedom for the free vibration analysis of antisymmetric angle-ply plates. Composite Structures 2008; 82(2): 209-216.
[19] Kheirikhah MM, Khalili SMR, Malekzadeh Fard K. Biaxial buckling analysis of soft-core composite sandwich plates using improved high-order theory. European Journal of Mechanics A/Solids 2012; 31(1): 54-66.
[20] Di Sciuva M, Icardi U. Numerical assessment of the core deformability effect on the behavior of sandwich beams. Composite Structures 2001; 52(1): 41-53.
[21] Rao MK, Desai YM. Analytical solutions for vibrations of laminated and sandwich plates using mixed theory. Composite Structures 2004; 63(3-4): 361-373.
[22] Dafedar JB, Desai YM, Mufti AA. Stability of sandwich plates by mixed, higher-order analytical formulation. International Journal of Solids and Structures 2003; 40(17): 4501-4517.

[23] Moreira RAS, Dias Rodrigues J. A layerwise model for thin soft core sandwich plates. Computers and Structures 2006; 84(19-20): 1256-1263.

[24] Di Sciuva M. Bending, vibration and buckling of simply supported thick multilayered orthotropic plates: an evaluation of a new displacement model. Journal of Sound and Vibration 1986; 105(3): 425-442.

[25] Di Sciuva M. Multilayered anisotropic plate models with continuous interlaminar stresses. Composite Structures 1992; 22(3): 149-167.

[26] Di Sciuva M. Development of an anisotropic, multilayered, shear-deformable rectangular plate element. Computers & Structures 1985; 21(4): 789-796.

[27] Di Sciuva M. A general quadrilateral multilayered plate element with continuous interlaminar stresses. Computers & Structures 1993; 47(1): 91-105.

[28] Di Sciuva M. A third-order triangular multilayered plate finite element with continuous interlaminar stresses. International Journal for Numerical Methods in Engineering 1995; 38(1): 1-26.

[29] Di Sciuva M., Icardi U., Villani M. Failure analysis of composite laminates under large deflection. Composite Structures 1998; 40(3-4): 239-255.

[30] Xiaohui R., Wanji C. Free vibration analysis of laminated and sandwich plates using quadrilateral element based on an improved zig-zag theory. Journal of Composite Materials 2011; 45(21): 2173-2187.

[31] Pandit MK, Sheikh AH, Singh BN. Analysis of laminated sandwich plates based on an improved higher order zigzag theory. Journal of Sandwich Structures and Materials 2010; 12(3): 307-326.

[32] Pandit MK, Sheikh AH, Singh BN. Buckling of laminated sandwich plates with soft core based on an improved higher order zigzag theory. Thin-Walled Structures 2008; 46(11): 1183-1191.

[33] Tessler A, Di Sciuva M, Gherlone M. Refinement of Timoshenko beam theory for composite and sandwich beams using zigzag kinematics. Technical Report NASA/TP-2007-215086, December 2007.

[34] Tessler A, Di Sciuva M, Gherlone M. A refined zigzag beam theory for composite and sandwich beams. Journal of Composite Materials 2009; 43(9): 1051 – 1081.

[35] Tessler A, Di Sciuva M, Gherlone M. Refined Zigzag Theory for laminated composite and sandwich plates. Technical Report NASA-TP-2009-215561, 2009.

[36] Tessler A, Di Sciuva M, Gherlone M. A consistent refinement of first-order shear deformation theory for laminated composite and sandwich plates using improved zigzag kinematics. Journal of Mechanics of Materials and Structures 2010; 5(2): 341-367.

[37] Di Sciuva M, Gherlone M, Tessler A. A robust and consistent first-order zigzag theory for multilayered beams, in: Gilat R, Banks-Sills L, editors. Advances in Mathematical Modelling and Experimental Methods for Materials and Structures: The Jacob Aboudi Volume, Springer, New York, 2010, pp. 255 - 268.

[38] Versino D. Refined theories and discontinuous Galerkin methods for the analysis of multilayered composite structures. Ph.D. thesis, Politecnico di Torino, Italy, 2012.

[39] Tessler A, Di Sciuva M, Gherlone M. Refined zigzag theory for homogeneous, laminated composite, and sandwich plates: a homogeneous-limit methodology for zigzag function selection. Technical Report NASA/TP-2010-216214, January 2010.

[40] Tessler A, Di Sciuva M, Gherlone M. A homogeneous limit methodology and refinements of computationally efficient zigzag theory for homogeneous, laminated composite, and sandwich plates. Numerical Methods for Partial Differential Equations 2011; 27(1): 208 – 229.

[41] Gherlone M, Tessler A, Di Sciuva M. C^0 beam elements based on the refined zigzag theory for multilayered composite and sandwich laminates. Composite Structures 2011; 93(11): 2882 – 2894.

[42] Oñate E, Eijo A, Oller S. Simple and accurate two-noded beam element for composite laminated beams using a refined zigzag theory. Computer Methods in Applied Mechanics and Engineering 2012; 213-216(1): 362-382.

[43] Versino D, Gherlone M, Mattone M, Di Sciuva M, Tessler A. An efficient, C^0 triangular elements based on the Refined Zigzag Theory for multilayered composite and sandwich plates. Composites Part B: Engineering 2013; 44B(1): 218 – 230.

[44] Birman V, Bert CW. On the choice of shear correction factor in sandwich structures. Journal of Sandwich Structures and Materials 2002; 4: 83-95.

[45] Gherlone M. On the use of zigzag functions in equivalent single layer theories for laminated composite and sandwich beams: a comparative study and some observations on external weak layers, accepted for publication on Journal of Applied Mechanics; 2013.

[46] Chueng-Yuan C. Nonlinear analysis of plates, McGraw-Hill Book Company, 1980.

[47] Reddy JN. Mechanics of laminated composite plates. Theory and analysis, CRC Press, Inc., 1997.

[48] Brush DO, Almroth BO. O. Buckling of Bars, Plates, and Shells, McGraw-Hill Book Company, 1975.

[49] Aiello MA, Ombres L. Buckling load design of sandwich panels made with hybrid laminated faces and transversely flexible core. Journal of Sandwich Materials and Structures 2007; 9(5): 467-485.

[50] Chakrabarti A, Sheikh AH. Buckling of laminated sandwich plates using an efficient plate model. International Shipbuilding Progress 2007; 54(1) 63-81.
[51] Khatua TP, Cheung YK. Stability analysis of multilayer sandwich structures. AIAA Journal 1973; 11(9): 1233-1234.
[52] Yuan WX, Dawe DJ. Overall and local buckling of sandwich plates with laminated faceplates, part II: applications. Computer Methods in Applied Mechanics and Engineering 2001; 190(40-41): 5215-5231.
[53] Giglio M, Manes A. Study of crack propagation in sandwich panels (Al Nomex). In: Proceedings of 34th National Conference of Italian Association for Stress Analysis, Milan, September 2005, (in Italian).
[54] Pagano NJ. Exact solutions for composite laminates in cylindrical bending. Journal of Composite Materials 1969; 3(3): 398-411.
[55] Ferreira AJM. A formulation of multiquadric radial basis function method for the analysis of laminated composite plates. Composite Structures 2003; 59(3): 385-392.
[56] Srinivas S, Rao AK. Bending, vibration and buckling of simply supported thick orthotropic rectangular plates and laminates. International Journal of Solids and Structures 1970; 6(11): 1463-1481.
[57] Rao MK, Scherbatiuk K, Desai YM, Shah AH. Natural vibration of laminated and sandwich plates. Journal of Engineering Mechanics 2004; 130(11) 1268-1278.
[58] Kulkarni SD, Kapuria S. Free vibration analysis of composite and sandwich plates using an improved discrete Kirchhoff quadrilateral element based on third-order zigzag theory. Computational Mechanics 2008; 42: 803-824.
[59] Di Sciuva M, Icardi U. On modeling of global and local response of sandwich plates. Journal of Sandwich Structures and Materials 2000; 2(4): 350-378.